CHAPTER 3

Screening and selection of candidate microalgae based on coal mine effluent bioremediation and thermal properties assessment*

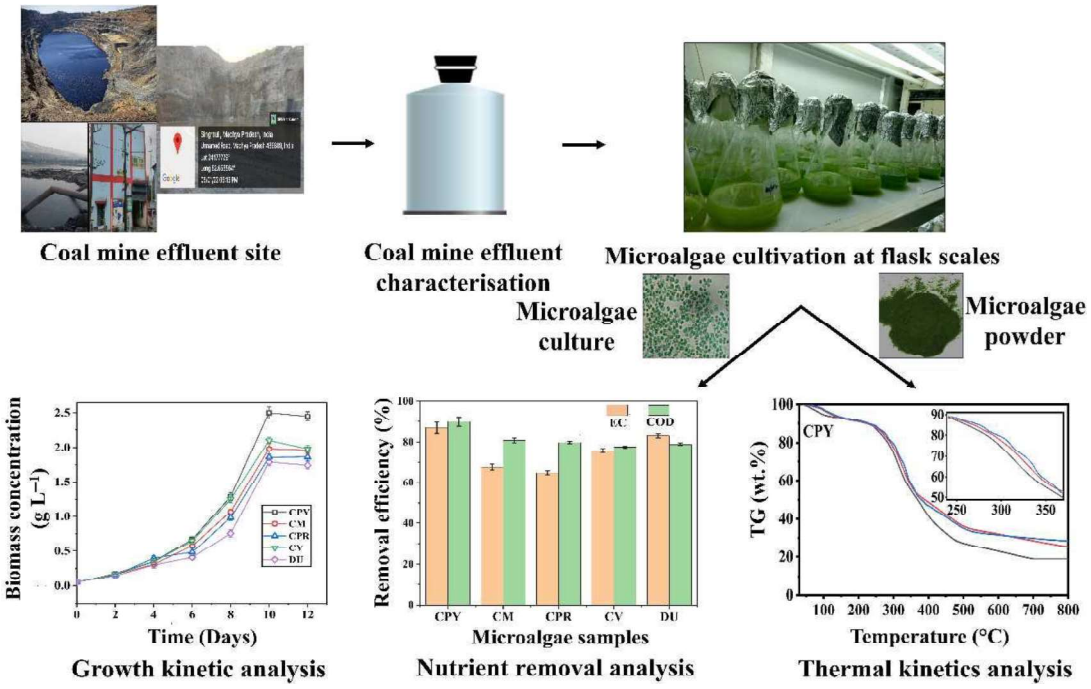

*Part of the work is published in **Shweta Rawat and Sanjay Kumar (2023c)** Thermal response estimation of de-oiled fresh and marine microalgae based on pyrolysis kinetic studies and deep neural network modeling. BioEnergy Research. 17, 570-586.

Abstract

Present chapter focuses on screening and selection of candidate microalgae to meet the desired objectives of coal mine effluent treatment and biofuel production. Freshwater microalgae strains, *C. pyrenoidosa, C. minutissima* and marine microalgae strains, *Dunaliella* sp. and *C. vulgaris* is utilized for CME treatment. To perform microalgae growth and desalination experiments, NSCME is prepared by adding MBG-11 chemicals in CME. A systematic screening of candidate microalgae is conducted based on growth kinetics, nutrient removal, fuel characteristic analysis, and thermal analysis of NSCME grown microalgae. According to growth kinetics results *C. pyrenoidosa* showed maximum growth potential amongst all five microalgae strains with μ_{net} of 0.33 d^{-1}. On the other hand, nutrient removal is investigated in terms of % salinity removal and % COD removal in both CME and NSCME medium. The maximum EC removal efficiency of *C. pyrenoidosa* (86.9 %) is very close to *Dunaliella* sp. (83 %) in NSCME as nutrient medium. The fresh microalgae *C. pyrenoidosa* showed COD removal (%) of 85.2 % in CME and 89.8 % in NSCME. Towards, fuel characteristic analysis, proximate and ultimate experiments are conducted to screen suitable de-oiled microalgae biomass as pyrolysis feedstock. Further, thermal behavior and kinetic analysis of de-oiled microalgae biomass are performed. In present study, model-fitted Coats Redfern (CR) and model-free distributed activation energy model (DAEM) showed apparent E_a of *C. pyrenoidosa*, *C. minutissima*, *C. protothecoides*, *C. vulgaris* and *Dunaliella* sp. as 55.87±11.16, 56.09±6.32, 46.58±5.55, 55.26±13.14 and 68.09±10.62 kJ/mol respectively. Finally, one-dimensional convolutional neural network (Conv1D) and long short-term memory (LSTM)-based Conv1D-LSTM model is established to predict microalgal pyrolysis data, which encourages artificial intelligence (AI) application in microalgae pyrolysis studies.

3.1. Background

This chapter focuses on the treatment of mine water discharged during coal mine excavation, rich in salt and trace metal ions. In between rising challenges concerning clean water availability, desalination is the most effective technology to target brackish groundwater, coal mine water, produced water, and seawater resources to reduce salt and other mineral components and provide clean water to water stress regions of the world (Demessie et al., 2019). Emerging desalination technologies as electrodialysis, reverse osmosis, membrane distillation, forward osmosis, multi-stage flash distillation, and multiple-effect distillation hold high water treatment capacity correlated with high energy consumption (Sharan et al., 2022). To replace these energy intensive desalination technologies, lower energy associated desalination processes, more specifically biodesalination, is considered an innovative technology. In bio-desalination, microalgae assisted salinity removal offers more energy-efficient, sustainable and environmentally feasible long-term wastewater management (Esmaeili et al., 2023). Following sustainable practices in coal mining, water footprint of mining may be reduced by applying biological wastewater treatment methods to treat CME for drinking/irrigation purposes (Levett et al., 2023). Amongst all green processes, microalgal platforms to treat mine water and desalination is considered as potential solution due to (i) microalgae cultivation capability in different types of wastewater facilities, (ii) efficient pollutant removal from water bodies, (iii) carbon capture potential of microalgae biomass, (iv) high value biomass, bio-fuel and metabolites production along with water treatment (Mirzaei et al., 2024).

In recent years, the desalination capability of different microalgae species such as *C. vulgaris* (Barahoei et al., 2021), *D. salina* (Mirzaei et al., 2024) and species from the genera *Scenedesmus*, *Desmodesmus*, *Chlorella* and *Chlorococcum* (Figler et al., 2019) are

investigated. The microalgae assisted wastewater treatment facilitates sustainable, low-cost processing technology for efficient salt ions/trace elements removal and microalgal biomass production for biofuels and other high value biochemicals (Mirzaei et al., 2024). In this direction, microalgal consortia (*S. bijugatus*, *Oscillatoria*, *Nannochloropsis* sp., *Chlorella* sp., *C. reinhardtii* and *Oscillatoria*) is investigated to treat sewage wastewater with heavy metal removal efficiency of 85.06% Cu, 98.2% Pb, 99.6% Cd, 75.2% Cr along with biomass concentration of 1.53 g L^{-1} and lipid content of 31.33% (Sharma et al., 2021).

Following the screening of candidate microalgae based on CME bioremediation, the evaluation of thermal properties of particular de-oiled microalgae feedstock with kinetics and energy analysis is also important for further bio-fuel application. In this direction, thermal characterization of de-oiled fresh and marine microalgae feedstocks was conducted based on fuel characterization, pyrolysis kinetics and activation energy (E_a) estimation. Both model-fitted Coats Redfern (CR) and model-free Distributed activation energy model (DAEM) approach were applied for reliable and consistent analysis of kinetic mechanism and E_a. Different data discrepancies issues are reported during TG investigations such as high sensitivity to heating rate, differences in thermal lag, compositional differences in biomass sample, and gas flow rate variation (Escalante et al., 2022). Targeting these issues and verifying the reliability of thermogravimetry experiments with improved consistency of data acquisition, a DNN model was designed to predict the high accuracy of the thermal decomposition of microalgae.

Overall, in view of the simultaneous application of candidate microalgae for CME treatment and bio-fuel production, present chapter deals with screening of fresh and marine microalgae cultures cultivated in NSCME based on (i) nutrient removal and growth kinetics, (ii) fuel characteristic analysis, (iii) thermal decomposition analysis and (iv) E_a estimation. Additionally, a new hybrid DNN model was designed to predict and verify TGA

data of de-oiled microalgae pyrolysis. As an outcome of present study, a systematic screening of fresh and marine microalgae is accomplished to achieve the most suitable candidate microalgae to be applied for simultaneous treatment of CME and bio-fuel production.

3.2. Materials and methods

3.2.1 Microalgae and culture condition

Freshwater microalgae strains, *C. pyrenoidosa* (NCIM 2738), *C. protothecoides* (NCIM 5527), *C. minutissima* (procured from Indian Agricultural Research Institute, India) and marine microalgae strains, *Dunaliella* sp. (BDU 10113) and *C. vulgaris* (BDUG D003) were utilized for CME treatment. Microalgae cultures were maintained in BG-11 medium consisting of $NaNO_3$ (1.5 g L^{-1}), $MgSO_4 \cdot 7H_2O$ (0.075 g L^{-1}), K_2HPO_4 (0.04 g L^{-1}), $CaCl_2 \cdot 2H_2O$ (0.036 g L^{-1}), Na_2CO_3 (0.02 g L^{-1}), citric acid with ferric ammonium citrate (0.006 g L^{-1} and 0.006 g L^{-1}), EDTA (0.001 g L^{-1}) and microelement solution of $MnCl_2 \cdot H_2O$ (1.81 g L^{-1}), H_3BO_3 (2.86 g L^{-1}), $CuSO_4 \cdot 5H_2O$ (0.079 g L^{-1}), $ZnSO_4 \cdot 7H_2O$ (0.222 g L^{-1}), $Co(NO_3)_2 \cdot 6H_2O$ (0.049 g L^{-1}) and $Na_2MoO_4 \cdot 2H_2O$ (0.39 g L^{-1}) as mentioned in previous study (Pandey et al., 2019). The cultured cells were grown in a photo cabinet at a temperature of 28 ± 2 °C, light intensity of 222.00 µmol photon/m^2/s under a light-dark period of 16:8 h (Pandey et al., 2019). During microalgae cultivation, the morphology of cells was investigated using a fluorescent microscope (Olympus CKX53) at regular time interval according to Bellinger and Sigee (2015).

3.2.2 Coal mine water collection, characterization and microalgae habitation

The CME was sampled from the coal main section at Singrauli coalfield (latitude 24.177729°N and longitude 82.65884°E), Madhya Pradesh, India, by following a standard water sampling process (APHA, 1989). As a pre-processing step, suspended particles of coal were removed from CME through filtration operation. To perform microalgae growth

and desalination experiments, NSCME was prepared by adding MBG-11 chemicals in CME. The chemical composition of MBG-11 is identical to BG-11 except Na component that is replaced with K component (Barahoei et al., 2021). The media composition of BG-11 and MBG-11 is presented in Appendix Table A.1 and Appendix Table A.2 respectively. The physicochemical characterization of CME and NSCME was determined by following the standard water and wastewater analysis methods by the American Public Health Association (APHA, 1989). Further, pH was determined by using a bench top pH meter (Eutech, pH 700, Thermo Fisher Scientific, Malaysia). Inductively coupled plasma mass spectrometry (ICP-MS) analysis was conducted using ICP-OES (Perkin Elmer, Shelton, US) to determine heavy metals in the CME.

To acclimatize the microalgae samples, active fresh and marine microalgae cultures were shifted from BG-11 media to CME and NSCME media sequentially for 10 days at control conditions mentioned in Section 3.2.1. All experiments were conducted in a 250 ml flask with 100 ml working volume in triplicate. For a consistent growth profile study, all flasks were inoculated with freshly grown microalgae cultures having an optical density of 2.0 at 680 nm wavelength and inoculum size of 10% (v/v) (Prajapati et al., 2014a).

3.2.3 Microalgae harvesting and pretreatment for thermal properties estimation

Following 15 days of batch cultivation in NSCME, microalgae biomass was harvested by applying high-speed continuous centrifugation at 2549×g rcf for 8 min. Then, centrifuged biomass was washed thrice with deionized water. Microalgae biomass was dried in an oven at 70 °C for three h and kept in a desiccator for further analysis. Total lipid from the dried algal powder was extracted with chloroform: methanol (1:2, v/v), as mentioned in Bligh and Dyer's method (Bligh et al., 1959). The de-oiled residual microalgae biomass was sun-dried for two weeks to remove excess moisture naturally before pulverization. The pulverized microalgae samples were sieved with a laboratory test micro sieve of 63 μm (American society for testing materials – ASTM mesh no. 230) to

minimize size variation and provide homogenous ignition during thermochemical conversion (Yap et al., 2022). The dried and pulverized de-oiled microalgae samples was kept in desiccator for further utilization to evaluate thermal properties.

3.2.4 Screening of fresh and marine algal isolates based on cell growth and nutrient removal

Towards integrated application for CME treatment and bio-fuel production, a systematic screening of candidate microalgae was conducted based on growth kinetics, nutrient removal, fuel characteristic analysis, and thermal analysis of NSCME grown microalgae. The selection flow chart of candidate microalgae for CME treatment and bio-fuel production is represented in Fig. 3.1.

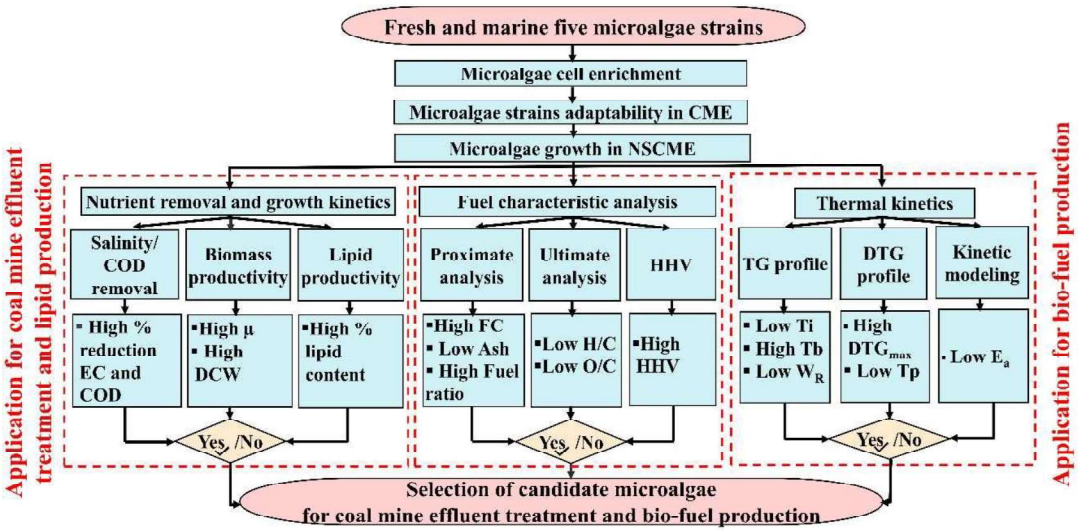

Fig. 3.1 Selection flow chart of candidate microalgae for coal mine effluent treatment and bio-fuel production. EC: Electric conductivity; COD: Chemical oxygen demand; μ: Specific growth rate, DCW: Dry cell weight; TDS: Total dissolved solid; FC: Fixed carbon; HHV: High heating value; Ti: Ignition temperature; Tb: Burn out temperature; W_R: Residual weight (%); DTG_{max} : Maximum decomposition rate; Tp : Peak temperature; E_a : Activation energy.

The candidate microalgae was assessed based on its ability to grow in NSCME followed by growth rate and nutrient removal potential. To acclimatize, microalgae cultures were shifted from BG-11 media to CME and NSCME media sequentially under

temperature of 28 ± 2 °C and light intensity of 222.00 µmol photon/m^2/s at mentioned light-dark cycle of 16:8 h for 12 days. Further, all microalgae cultures were transferred to a 500 ml flask with working volume 300 ml. The flasks were inoculated with active algal culture having an optical density of 2.0 at 680 nm ($OD_{680\ nm} \approx 2.0$), and the inoculum size was kept at 10% (v/v). The samples were withdrawn regularly to determine growth kinetic parameters, defined as specific growth rate (µ) and doubling time (t_d). The nutrient removal parameters, i.e., chemical oxygen demand (COD), electric conductivity (EC), and salinity reduction, were also determined at the same interval. Finally, the candidate microalgae was screened based on maximum growth (µ) and maximum salinity reduction (% EC removal).

3.2.4.1 Microalgae screening based on growth kinetics analysis

Microalgae biomass growth for fresh and marine microalgae was determined by a spectrophotometric method using the respective correlation equations derived from the dry cell weight and $OD_{680\ nm}$ for each strain. To measure absorbance of these samples at 680 nm, UV/visible spectrophotometer (UV/VIS Lambda 365, PerkinElmer, USA) was used. The dry cell weight (DCW) was measured gravimetrically by centrifugation of cultures at relative centrifugal force of 2459 g rcf for 10 min followed by oven drying at 60 °C till the constant weight attainment as reported previously (Pandey et al., 2019).

In growth profile, µ (d^{-1}) and t_d (d) were determined by following Eq. 3.1 and Eq. 3.2 respectively:

$$\mu = \frac{ln\left(\frac{W_t}{W_0}\right)}{\Delta t} \tag{3.1}$$

$$t_d = \frac{\ln(2)}{\mu} \tag{3.2}$$

Where, W_0 and W_t are the initial and final dry cell weight at the start and end of the batch cultivation.

The lipid content (%) was determined according to Eq. 3.3:

$$Lipid\ content\ (LC\ \%) = \frac{(LC_f - LC_i) \times V_t}{V_a} \times 100 \tag{3.3}$$

Where, LC_f and LC_i are the final and initial weight of the lipid content in mg, respectively; V_a and V_t are specified as total volumes of aliquot and organic layer in mL.

3.2.4.2 Microalgae screening based on salinity and chemical oxygen demand (COD) removal

High to mild salinity level in CME is considered as a sensitive parameter with aspect of irrigation because high salinity can create hinderance for the crop to adsorb nutrients and cause specific ion toxicity (Mansilha et al., 2021). Salinity was monitored during microalgae cultivation by measuring electrical conductivity (EC) using an electrical conductivity meter (Eutech CON 700, Thermo Fisher Scientific, Malaysia). The COD was determined using COD analyzer with digester (Uniphos, Gujrat, India). The salinity reduction was calculated by using Eq. 3.4.

$$Salinity\ removal\ \% = \frac{100(EC_i - EC_f)}{EC_i} \quad (3.4)$$

Where, EC_i and EC_f are considered as initial and final EC values of the culture medium, respectively.

Further, COD removal % was calculated by using Eq. 3.5.

$$COD\ removal\ \% = \frac{100(C_f - C_i)}{C_i} \quad (3.5)$$

Where, C_f and C_i are considered as final and initial COD values of the culture medium, respectively.

3.2.4.3 Elemental and biochemical analysis of biomass

The elemental composition of dried and powdered algal biomass was determined using a CHN628 elemental analyser (LECO, Michigan, USA) and the ASTM D5373-14 standard. The volatile matter and ash content of algal biomass was assessed following ASTM D7582-15 standard as mentioned in our earlier reported paper (Rawat and Kumar, 2023a). To understand the structural features and presence of various functional groups in microalgae biomass and lipid, Fourier transform infrared spectroscopy (FTIR) was

conducted by Cary 630 FTIR (Agilent, California, USA) as mentioned in our previously reported study (Rawat and Kumar, 2023a). The high heating value (HHV) as well as low heating value (LHV) of microalgal biomass was calculated on dry basis (db) in MJ Kg^{-1} based on CHNO analysis using Eq. 3.6–3.7 as reported by Miranda et al. (2018).

$$HHV = 0.3383 \times C + 1.422 \times \left(H - \frac{O}{8}\right) \quad (3.6)$$

$$LHV = HHV - 2.447 \times \left(\frac{H}{100}\right) \times 9.011 \quad (3.7)$$

Where, C, H and O are defined as weight percentages of carbon, hydrogen and oxygen in the biomass, respectively.

3.2.5 Microalgae screening based on thermal characteristic analysis

The thermal properties of de-oiled microalgae were analyzed based on fuel characteristic analysis, thermal decomposition analysis, and E_a, as well as other thermodynamic properties estimation.

3.2.5.1 Fuel characteristic analysis of microalgae samples

Pulverized and sieved microalgae samples were characterized through proximate analysis and performed according to the standard protocol (ASTM D7582-15). Elemental analysis was conducted in a CHN628 elemental analyzer (LECO, Michigan, USA) as per the standard method (ASTM D5373-14). The HHV of samples was conducted in Parr 6100 oxygen bomb calorimeter (Parr Instrument, USA) according to the standard of ASTM D5865-13.

For statistical analysis of different microalgae fuel characteristic variables, Spearman's rank correlation was performed using IBM SPSS statistics 29.0 to correlate the fuel characteristic variables of different microalgae samples. The Spearman's rank correlation coefficient (r_s) is a nonparametric or distribution free rank statistic applied to determine the strength of association between two variables (Meng et al., 2023). In the present study, the two prominent fuel characteristics (fuel ratio and HHV) were individually

correlated with important proximate analysis variables such as fixed carbon, volatile matter and ash. Based on the strength of the association between variables, r_s lies between –1 to 1. The correlations were considered significant in this study with an absolute value of $r_s \geq 0.70$ at p-value ≤ 0.05.

Moreover, parametric one-way analysis of variance (ANOVA) was used to determine the statistical significance of all fuel characteristic variables for different microalgae groups using IBM SPSS statistics 29.0. One-way ANOVA under unequal variances was used to find whether the mean values of independent variables between different microalgae groups differed significantly or not.

3.2.5.2 Thermogravimetric and Fourier transform infrared analysis

The thermal decomposition analysis of both fresh and marine microalgae was investigated in a TGA-50 thermogravimetric analyzer (Shimadzu, Kyoto, Japan). Initially, temperature calibration was completed at a set heating rate by analyzing the TG signal of the melting peak temperature of pure substances: Zn (427.8 ºC), Sn (235.4 ºC), Au (1073.9 ºC), and Al (686.2 ºC) using similar crucible (Alumina) and set conditions. Baseline correction was completed in an empty crucible at an identical heating rate by applying nitrogen and oxygen environment. After that, pulverized and dried samples (approximately 10 mg) were placed in TGA and heated from ambient temperature to 800 ºC. Three different heating rates, 10, 20 and 30 ºC/min were used to analyze the thermal and kinetic analysis and the effect of heating rate upon thermal decay (Das et al., 2015). Nitrogen was used as a purge gas at a 100 ml/min flow rate to maintain an inert environment and establish essential pyrolysis conditions within the system. Each experiment set was repeated three times to minimize the experimental error.

The presence of functional groups in fresh and marine microalgae was determined using a Fourier transform infrared (FTIR) analysis. Dried microalgae samples were mixed with KBr and finely ground in an agate mortar. The resulting mixture was compressed in the form of a transparent tablet. The FTIR spectra of prepared tablets were measured by Cary 630 FTIR (Agilent, California, USA) in the region of 500–4000 cm. The detailed analysis of TGA and FTIR curves were performed using Origin 9.8 software.

3.2.5.3 Kinetic analysis of microalgae biomass pyrolysis

Microalgae biomass pyrolysis kinetic analysis was performed using the model-fitted CR and model-free DAEM methods. The kinetic parameters were studied by curve fitting analysis using Origin 9.8 software.

As a model-fitting approach, the CR method was applied to calculate the kinetic decomposition of the fresh and marine microalgae according to Eq. 3.8.

$$ln\left[\frac{g(x)}{T^2}\right] = ln\left[\frac{AR}{\beta E_a}\left(1-\frac{2RT}{E_a}\right)\right]-\frac{E_a}{R}\frac{1}{T} \quad (3.8)$$

Where A, R, β, T, and E_a are defined as the pre-exponential factor (min^{-1}), universal gas constant (8.314 J mol^{-1} K^{-1}), heating rate (ºC/min), absolute temperature (K) and E_a (kJ/mol), respectively during pyrolysis. The plotting of $ln\left[\frac{g(x)}{T^2}\right]$ vs. $1/T$ provides E_a and A data (Raza et al., 2022).

The conversion degree (α) and rate constant (k) during pyrolysis are expressed as Eq. 3.9 and Eq. 3.10, respectively.

$$\alpha = \frac{m_0 - m_i}{m_0 - m_f} \quad (3.9)$$

$$k = A\ exp\left(\frac{-E_a}{R\,T}\right) \quad (3.10)$$

Where m_0, m_i and m_f represent the original mass, instantaneous mass at any time t and final mass of the sample, respectively.

The model-fitted approach of CR has been used with different solid-state models to determine the kinetic behavior of fresh and marine microalgae samples by using eight reaction mechanisms under three categories. In these major categories, the chemical reaction mechanism model calculates homogeneous pyrolytic chemical reactions based on first, second and third order reactions, represented by O1, O2 and O3, respectively.

Secondly, dimensional diffusion models D1, D2 and D3 are applied based on diffusion phenomenon. Finally, random nucleation and nuclei growth models based on the Avraami Erofeev equation represent N1 and N2. The mathematical expression of g(x) applied for biomass pyrolysis kinetic model is expressed in Table 3.1.

Table 3.1 Mathematical expressions of f(x) and g(x) for the most applied solid-state kinetic models.

Model	Symbol	Differential form (f(x))	Integral form (g(x))
Based on chemical reaction			
First order	O1	$(1-\alpha)$	$-\ln(1-\alpha)$
Second order	O2	$(1-\alpha)^2$	$-1+(1-\alpha)^{-1}$
Third order	O3	$(1-\alpha)^3$	$[-1+(1-\alpha)^{-2}]/2$
Based on diffusion mechanism			
One- dimensional diffusion Plane symmetry	D1	$\alpha^{-1}/2$	α^2
Two- dimensional diffusion Cylindrical symmetry	D2	$[-\ln(1-\alpha)]^{-1}$	$\alpha+(1-\alpha)\ln(1-\alpha)$
Three-dimensional diffusion Spherical symmetry	D3	$3(1-\alpha)^{2/3}[1-(1-\alpha)^{1/3}]^{-1/2}$	$[1-(1-\alpha)^{1/3}]^2$
Based on Avraami Erofeev equation			
Random nucleation and nuclei growth	N1	$2(1-\alpha)[-\ln(1-\alpha)]^{1/2}$	$[-\ln(1-\alpha)]^{1/2}$
Random nucleation and nuclei growth	N2	$3(1-\alpha)[-\ln(1-\alpha)]^{1/3}$	$[-\ln(1-\alpha)]^{1/3}$

α: mass conversion ratio.

In between these approaches (Table 3.1), the chemical reaction mechanism model is interpretable based on classical chemical kinetic theory, assuming that biomass pyrolysis is controlled by chemical reactions only (Postawa et al., 2022). Oppositely, the diffusion mechanism is governed by pore structure and particle size of biomass and depends upon intra-particle heat and mass transfer (Postawa et al., 2022). On the other hand, the Avraami Erofeev equation describes the solid transformation of one phase from another during biomass pyrolysis by the growth of nuclei forming randomly in the parent phase.

A model-free approach, DAEM, was applied to revalidate the pyrolysis kinetics parameters. The basic assumption behind DAEM is the existence of infinite parallel first-order reactions during pyrolysis, which are independent and irreversible. The different E_a for each reaction can be calculated by DAEM mathematical expression shown in Eq. 3.11.

$$1 - \frac{V}{V^*} = \int_0^\infty exp\,(-A\,dx \int_0^t e^{-E_a/RT}\,dt\,) f(E) d(E) \tag{3.11}$$

Where V and V^* are volatile content at temperature T and effective volatile content, respectively. The $f(E)$ denotes the changes in E_a during pyrolysis reactions and A is the frequency factor corresponding to the E_a values. To minimize the prior assumptions concerned with $f(E)$ and $k_0(E)$, Miura and Maki (1998) presented a simpler and more accurate method through the integration of the Arrhenius plot as expressed in Eq. 3.12.

$$ln\left(\frac{\beta}{T^2}\right) = ln\left(\frac{AR}{E_a}\right) + 0.6075 - \frac{E_a}{R}\frac{1}{T} \tag{3.12}$$

At particular v/v^* value and β, the Arrhenius plot between $ln\,(\beta/T^2)$ and $1/T$ in Eq. 3.12 gives parallel straight lines to calculate the E_a and A from the slope and intercept, respectively. Therefore, this simplified Eq. 3.12 of the DAEM approach is highly applicable to analyzing the weight loss curves of microalgae samples at different heating conditions.

3.2.5.4 Thermodynamic properties estimation of different microalgae biomass

The thermodynamic parameters ΔH, ΔS and ΔG were calculated using E_a and A estimated from the CR equation and DAEM model. Eq. 3.13–3.15 represents the correlations for calculating these thermodynamic properties.

$$\Delta H = E_a - RT \tag{3.13}$$

$$\Delta S = R \times ln\left(\frac{Ah}{kT_P}\right) \tag{3.14}$$

$$\Delta G = \Delta H - T_P \Delta S \tag{3.15}$$

Where, ΔH, ΔS, and ΔG are represented as a change in enthalpy, entropy and Gibbs free energy, respectively. Further, h and k correspond to Planck's constant (6.626×10^{-34} J/s) and Boltzmann constant (1.381×10^{-34} J/K). Tp is the DTG peak temperature (K).

3.2.5.5 Deep neural network data processing and model designing

The data was prepared by selection from the large experimental set of nearly 7000 data points of individual pyrolysis experiments at different heating rates (10–30 ºC/min). Machine learning algorithms converge faster when the different inputs are on a smaller scale. Therefore, data was normalized based on input features. The normalized data is randomly split into training and validation datasets in a 70:30 ratio. The validation dataset is further divided in 50:50 ratio for validation and test dataset.

The DNN model was designed to predict the thermal decomposition of fresh and marine microalgae. The One-dimensional convolutional neural network (Conv1D) – Long short-term memory (LSTM) layers were applied to simulate TG data of different heating rates at 10–30 ºC/min using an open-sourced application programming Interfaces Keras (version 2.11.0) and skilearn (version 1.2.0) on Jupyter notebook (version 6.4.8) using the python programming language (version 3.9.12). The model consisted of 1 input layer

(Conv1D), 4 hidden layers (Conv1D, LSTM, Dense-2) and 1 output layer to produce univariate output. Kernel size, activation function, and bias vector were key parameters of the 1D convolution layer. Kernel size specifies the length of the Conv1D window, which was set at 2. An advanced parametric rectified linear unit (PreLU) was used as an activation function by considering its better performance in solving the dead neuron problem and bias vector set as true. Max pooling1D function was applied for pooling operation on temporal data by setting pool size at 2. LSTM layer used tanh as an activation function, sigmoid as a recurrent activation function and bias vector set as true. The core dense hidden layer used a level2 (L2) kernel regulariser set at 0.01. The output layer used a linear activation function to predict univariate remaining mass %.

The designed model was compiled by defining the optimizer function, loss function and model metrics. Adam was used as an optimizer algorithm set at a learning rate of 0.001. Mean square error (MSE) was used as a loss function and mean absolute error (MAE) as a model metrics. The network's hyperparameters were tuned up during model training for the best performance. The model was trained with training data. Further, validation data was used to determine the performance of the loss function and model metrics. The MSE, root mean square error (RMSE), regression coefficient (R^2) and MAE were used to evaluate the DNN model performance according to Eq. 3.16 – 3.19 as reported in the literature (Garcia et al., 2020).

$$MSE = \frac{1}{N} \sum_{i=1}^{n} (\alpha_i - \hat{\alpha}_i)^2 \tag{3.16}$$

$$RMSE = \sqrt{\frac{1}{N} \sum_{i=1}^{n} (\alpha_i - \hat{\alpha}_i)^2} \tag{3.17}$$

$$R^2 = 1 - [\sum_{i=1}^{n} (\alpha_i - \hat{\alpha}_i)^2] / [\sum_{i=1}^{n} (\alpha_i - \bar{\alpha}_i)^2] \tag{3.18}$$

$$MAE = \frac{1}{N} \sum_{i=1}^{n} | \alpha_i - \hat{\alpha}_i | \tag{3.19}$$

Where, α_i , $\widehat{\alpha}_i$, and $\bar{\alpha}_i$ correspond to the experimental, predicted and average value of output.

3.3. Results and discussion

3.3.1 Physical and chemical characterization of coal mine effluent

The physical and chemical characteristics used to evaluate the water quality of CME collected from the coal main section at Singrauli coalfield is presented in Table 3.2. The results were compared to the water reuse guidelines of the United States Environmental Protection Agency (EPA) and the Food and Agriculture Organization (FAO). The present study focused on water reusability specifically for irrigation purposes in nearby coal mine area. The CME water was observed with neutral pH (7.96 ± 0.43) and moderate total dissolved solids (556 ± 5.5 mg L^{-1}). In comparison to FAO guidelines, CME showed high salinity (4.8±0.5 mS/cm), high nitrate (NO_3^{-1}) concentration (69 ± 0.5 mg L^{-1}) and high bicarbonate (HCO_3^{-1}) concentration (8.4 ± 0.5 mg L^{-1}). Utilizing CME water for irrigation may cause salinity hazards in soil that can create specific ion toxicity, eutrophication, delayed crop maturity and limits water uptake from the soil (Manshila et al., 2021).

Analysing major inorganic elements and trace metals by ICP-MS, it was observed that Na (250 ± 2.5 mg L^{-1}), Fe (7.5 ± 0.38 mg L^{-1}), Cu (2.01 ± 0.05 mg L^{-1}), Pb (0.65 ± 0.10 mg L^{-1}) and Cr (0.18 ± 0.007 mg L^{-1}) exceeded from water reusability limits of EPA and FAO standards (Table 3.2). Directly using this water for irrigation may cause high doses of trace metals in soil, hindering root to shoot nutrient transport and clogging to irrigation equipment (Lin et al., 2024). In strong agreement with previously reported studies, microalgae are considered the most efficient organisms capable of growing in nutrient rich wastewater and reducing the pollutant load in the water bodies (Chen et al., 2021). The N/P ratio of NSCME is approximately 7.99 (Table 3.2), which is appropriate for healthy growth of microalgae and near to other reported optimal N/P ratios of coal mine water.

Table 3.2 Physico-chemical characteristics of coal mine effluent and nutrient supplemented coal mine effluent.

Parameter	CME	NSCME	Permissible limits	
			EPA	FAO
Temperature (ºC)	21.5 ± 1.05	21.8 ± 2.0	ND	ND
pH	7.96 ± 0.43	7.8 ± 0.5	5-9	6.5-8.4
Total dissolved solids (mg L^{-1})	556 ± 5.5	586 ± 8.5	500	ND
TOC (mg L^{-1})	54 ± 0.25	61 ± 0.30	ND	ND
COD (mg L^{-1})	264 ± 0.54	285± 1.5	ND	ND
TN (mg L^{-1})	45.7 ± 2.87	48.2 ± 4.03	ND	ND
TP (mg L^{-1})	5.37 ± 0.37	6.03 ± 0.33	ND	ND
Salinity				
Electric conductivity (mS cm^{-1})	4.8 ± 0.50	5.2 ± 0.50	ND	< 0.7
Elements and Metals (mg L^{-1})				
Na	250 ± 2.5	250 ± 2.5	200	207
Mg	30.2 ± 0.05	38 ± 0.9	ND	0-60
Ca	28.3 ± 0.05	39 ± 0.5	ND	0-100
Fe	7.5 ± 0.38	8.78 ± 0.5	2.0	5.0
Mn	5.5 ± 0.45	6.01 ± 0.5	0.2	0.2
Cu	2.01 ± 0.05	2.05± 0.07	0.5	0.2
Zn	1.01 ± 0.15	1.07 ± 0.2	0.1	2.0
Ni	0.81 ± 0.18	0.83 ± 0.11	0.1	0.2
Pb	0.65 ± 0.10	0.65 ± 0.10	0.05	0.5
Cr	0.18 ± 0.007	0.18 ± 0.007	0.05	0.1
Cd	0.05 ± 0.008	0.05 ± 0.008	0.01	0.01
B	0.5 ± 0.005	0.91 ± 0.05	ND	0.7

CME: Coal mine effluent; NSCME: Nutrient supplemented coal mine effluent (NSCME); EPA: Environmental Protection Agency water reuse guidelines. FAO: Food and Agriculture Organization water reuse guidelines for irrigation suitability; ND: Not detected. The data are represented as mean value ± standard deviation (< 3%).

Hence, microalgae based low cost biological operation was utilized to treat CME and reduce the salinity as well as excess metal loading till irrigation permissible limit described by EPA and FAO guidelines. The NSCME was used to perform microalgae growth and effective desalination experiments. The physicochemical characterization of NSCME is presented in Table 3.2.

3.3.2 Growth and screening of potential microalgae in nutrient supplemented coal mine effluent

Fresh and marine microalgae strains were investigated with aspect of growth kinetics as well as nutrient removal in CME and NSCME to screen potential microalgae

for bioremediation of coal mine water. The cell growth of all microalgae strains was measured after 12 days of batch cultivation. The growth profiles of *C. pyrenoidosa*, *C. protothecoides, C. minutissima*, *C. vulgaris* and *Dunaliella* sp. cultivated in CME and NSCME are shown in Fig. 3.2. The growth profiles imply that microalgae strains are fully adapted to NSCME and show better growth in NSCME than CME. The biomass concentration (g L^{-1}) and further, μ (d^{-1}) / t_d (d) were estimated (according to section 2.5.1). Growth kinetics result interpretated that fresh microalgae, *C. pyrenoidosa* showed best growth in CME (1.01 g L^{-1}) and marine microalgae, *Dunaliella* sp., showed the lowest biomass concentration (0.6 g L^{-1}) in CME at the end of 10 d cultivation (Fig. 3.2a). After nutrient addition, enhanced microalgae growth can be observed for both fresh and marine microalgae. Fresh microalgae, *C. pyrenoidosa* showed 2.5 times more growth in NSCME than CME. In marine microalgae, *C. vulgaris* attained better adaptability in NSCME with cell growth 2.1 g L^{-1} than *Dunaliella sp.* with cell growth 1.8 g L^{-1} at the end of exponential phase (Fig. 3.2b). In NSCME, the highest μ_{net} (d^{-1}) of 0.33 and corresponding shortest t_d (d) of 2.1 is observed for *C. pyrenoidosa* as shown in Fig. 3.2b.

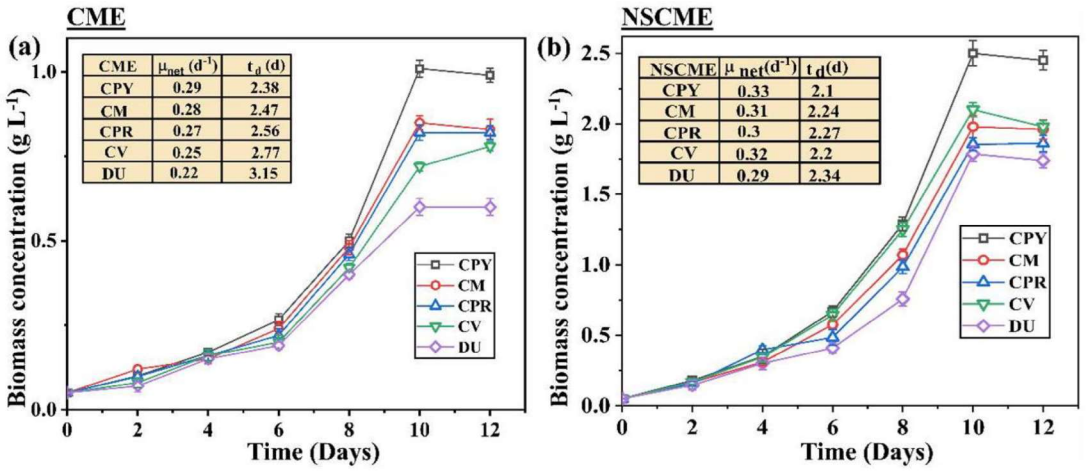

Fig. 3.2 Growth profiles of fresh and marine microalgae strains – *Chlorella pyrenoidosa* (CPY), *Chlorella minutissima* (CM), *Chlorella protothecoides* (CPR), *Chlorella vulgaris* (CV), *Dunaliella sp.* (DU) in (a) coal mine effluent (CME) (b) nutrient supplemented coal mine effluent (NSCME). μ_{net} (d^{-1}) : Specific growth rate; t_d (d) : Doubling time.

Investigating 12 days batch study in NSCME, all fresh and marine microalgae reached the stationary phase after 10 d. Further, nutrient removal was investigated in terms of % salinity removal and % COD removal in both CME and NSCME medium. EC is considered a necessary parameter for detecting salinity and is directly proportional to the amount of salinity (Barahoei et al., 2021). Further, COD may be regarded as an indirect measurement of all organic and inorganic nutrients in coal mine water. The nutrient removal efficiency (%) was determined during the batch cultivation period (Fig. 3.3a and b).

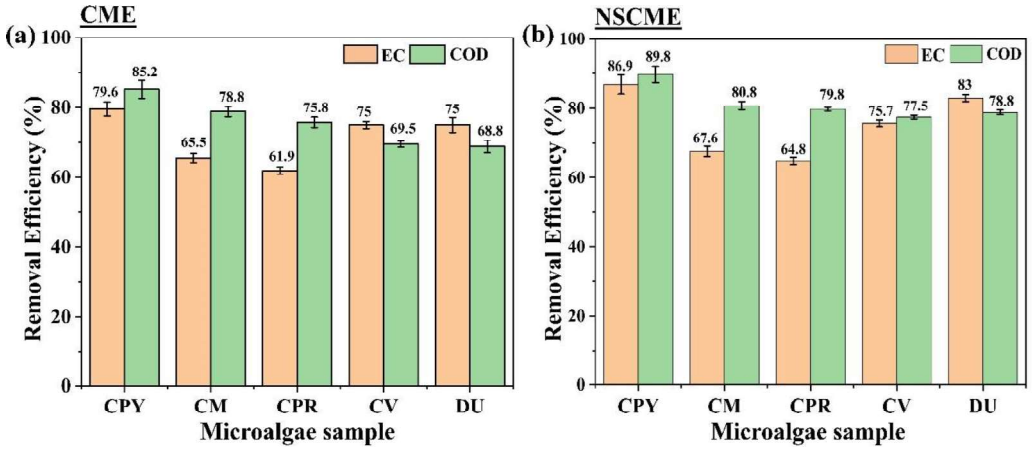

Fig. 3.3. Nutrient removal efficiency (%) of fresh and marine microalgae strains in (a) coal mine effluent (CME) (b) nutrient supplemented coal mine effluent (NSCME). CPY: *Chlorella pyrenoidosa*, CM: *Chlorella minutissima*, CPR: *Chlorella protothecoides*. CV: *Chlorella vulgaris* and DU: *Dunaliella* sp. EC (%): Electric conductivity, COD (%): Chemical oxygen demand.

In CME, fresh microalgae, *C. pyrenoidosa* showed maximum 79.6% EC removal efficiency which is close to marine microalgae, *C. vulgaris* and *Dunaliella* sp. showing identical 75% EC removal efficiency (Fig. 3.3a). All five microalgae strains showed variation in EC removal efficiency in the range of 86.9–64.8% in NSCME (Fig. 3.3b). The maximum EC removal efficiency of *C. pyrenoidosa* (86.9%) is very close to *Dunaliella* sp. (83%) in NSCME as a nutrient medium (Fig. 3.3b). The probable reason is marine microalgae show good salt tolerance potential and require high salt concentration for growth (Esmaeili et al., 2023). However, the NSCME shows moderate salinity as brackish water, which is more suitable for growing fresh water than marine microalgae.

3.3.3 Fuel characteristic analysis of fresh and marine microalgal biomass

Fuel characteristic analysis, such as proximate, ultimate, and HHV analysis, is fundamental to bioenergy application. These fuel characteristic parameters for fresh and marine microalgae species are summarized in Table 3.3.

Table 3.3 Basic fuel characteristics for freshwater and marine microalgae species.

Analysis	Freshwater microalgae			Marine microalgae	
	CPY	CM	CPR	CV	DU
Proximate analysis (mass %)					
Moisture content	4.94	6.18	5.98	3.18	2.50
Volatile matter	43.01	42.57	47.85	47.50	48.0
Fixed carbon	34.05	28.75	25.34	28.75	27.87
Ash	18.0	22.50	20.83	20.57	21.63
Mineral matter[a]	19.8	24.75	22.91	22.63	23.79
Pyrite[b]	8.30	12.59	9.24	4.86	7.27
Fuel ratio[c]	0.79	0.68	0.53	0.61	0.58
High heating value (HHV- MJ/kg)	18.60	16.63	16.25	17.41	17.17
Ultimate analysis (mass %)					
C	45.06	44.97	37.24	28.19	36.42
H	6.62	5.53	5.91	4.95	4.89
O	41.20	34.73	50.58	59.18	51.35
N	5.67	4.16	5.09	6.61	5.83
S	1.45	2.48	1.78	1.07	1.51
C/H	6.81	8.13	6.30	5.69	7.45
O/C	0.91	0.77	1.35	2.09	1.41
C/N	0.00	0.00	0.00	0.00	0.00

CPY *: Chlorella pyrenoidosa*; CM: *Chlorella minutissima*; CPR: *Chlorella protothecoides*; CV: *Chlorella vulgaris*; DU: *Dunaliella sp.*; [a]Mineral matter mass% = 1.10. (Ash mass %); [b]Pyrite = 130. (S mass% -0.30)/ Ash mass % ; [c]Fuel ratio = Fixed carbon/ Volatile matter. Mineral matter, pyrite, fuel ratio was calculated according to Jankovic et al. (2020). All observed values of responses were mean values of duplicates and standard deviation less than 3%.

The heating value (MJ Kg^{-1} dry weight) is described as total amount of heat energy released on complete combustion of a unit mass of microalgae (Pandey et al., 2019). The calculated HHV for *C. pyrenoidosa*, *C. minutissima*, *C. protothecoides*, *C. vulgaris* and *Dunaliella sp.* was 18.60, 16.63, 16.25, 17.41 and 17.17 MJ/kg, respectively. Similar to HHV, the fuel ratio was also found to be maximum for *C. pyrenoidosa* among different microalgae species. Ash content and volatile matter negatively impact the fuel characteristics such as HHV and fuel ratio. The ash content of microalgae biomass represents incombustible components deposited as slag, which requires additional heat

fluxes for burning. Fresh microalgae, *C. pyrenoidosa* showed minimum ash content (18.0 %) and comparatively low volatile content (43.01%). The fixed carbon of fuel feedstock was directly proportional to HHV, which was maximum for *C. pyrenoidosa* (34.05%) and minimum for *C. protothecoides* (25.34%). The energy content of the fuel is positively influenced by a high carbon-to-hydrogen ratio (C/H) and a low oxygen-to-carbon ratio (O/C) (Hossain et al., 2019). Further, *C. minutissima* shows maximum C/H and minimum O/C ratio. For, *C. pyrenoidosa*, both ratios, C/H (6.81) and O/C (0.91), lie in between. This O/C is very close to other reported values for *Chlorella* sp. (Phukan et al., 2011). The reported O/C ratio for agriculture residues (0.85), rice straw (0.96), pine sawdust (0.88) and switchgrass (0.87) are comparable with present study (0.77–2.09) (Kamble et al., 2019). Low S and low pyrite content are desirable as high S content causes rusting of the reactor surface (Jankovic et al., 2020). The microalgae species showed varying S content with 1.07% (*C. vulgaris*) to 2.48% (*C. minutissima*). According to elemental composition analysis, all five microalgal biomass have carbon (C) (45.06–28.19%), hydrogen (H) (6.62–4.89%), nitrogen (N) (6.61–4.16%) and oxygen (O) (59.18–34.73%) as major constituents (Table 3.3). The C/N of the microalgal biomass is observed in the range of 4.26–10.81% (Table 3.3). On 12 th day of batch cultivation, the lipid content (%, w/w) is observed as 31.5, 25.6, 23.8, 20.4 and 19.8 (mean values of triplicates and standard deviation less than 3%) in *C. pyrenoidosa*, *C. minutissima*, *C. protothecoides*, *C. vulgaris* and *Dunaliella* sp. respectively. The total lipid content (31.5%, w/w) in *C. pyrenoidosa* cultivated in NSCME is found to be significantly more than previously reported *Chlorella* sp. cultivated in tap water and waste water as shown in Table 3.4.

Table 3.4 Biomass characterization of fresh and marine microalgal cultures, cultivated in nutrient supplemented coal mine effluent.

Microalgae	Medium	Lipid (%, w/w)	Carbon (%, w/w)	Hydrogen (%, w/w)	Nitrogen (%, w/w)	Oxygen (%, w/w)	Heating value ($MJ\ Kg^{-1}$)		Empirical equation	References
							HHV	LHV		
Scenedesmus dimorphus	Synthetic waste water	32	51.16	10.24	2.58	8.94	30.28	28.022	$C_{23.09}H_{55.21}NO_{3.03}$	Faruque et al., (2023)
Scenedesmus sp.	Synthetic dairy effluent	30.7	51.28	5.01	7.72	29.42	19.24	19.13	$C_{7.76}H_{9.01}NO_{3.35}$	Pandey et al., (2019)
Chlorella sorokiniana	Sewage water	ND	64.24	12.08	5.02	18.56	35.74	33.07	$C_{15.28}H_{34.23}NO_{3.31}$	Lamba et al., (2023)
Chlorella pyrenoidosa	Tap water	13.7	45.90	5.95	5.55	14.95	21.33	20.02	$C_{8.16}H_{12.6}NO_{1.86}$	Prajapati et al., (2014a)
Chlorella minutissima	Tap water	16.3	41.54	5.85	7.02	19.24	18.95	17.66	$C_{6.87}H_{11.58}NO_{2.40}$	Prajapati et al., (2014a)
Chlorella thermophila	Dairy wastewater	27.5	47.51	9.21	7.04	36.24	22.72	20.69	$C_{7.86}H_{18.17}NO_{0.87}$	Mohanty et al., (2023)
Chlorella pyrenoidosa	Wastewater	25.3	48.32	7.45	4.65	39.19	19.96	18.39	$C_{12.19}H_{22.39}NO_{7.42}$	Satheesh et al., (2023)
Chlorella sorokiniana	Wastewater	26.2	45.5	7.14	5.12	41.65	18.14	16.56	$C_{10.37}H_{19.40}NO_{7.14}$	Satheesh et al., (2023)
Chlorella pyrenoidosa	NSCME	31.5	45.06	6.62	5.67	41.20	18.60	17.14	$C_{9.26}H_{16.23}NO_{6.36}$	Present study
Chlorella minutissima	NSCME	32.6	44.97	5.53	4.16	34.73	16.63	15.41	$C_{12.59}H_{18.45}NO_{7.31}$	Present study
Chlorella protothecoids	NSCME	23.8	37.24	5.91	5.09	50.58	16.25	15.13	$C_{8.539}H_{16.14}NO_{8.71}$	Present study
Chlorella vulgaris	NSCME	20.4	28.19	4.95	6.61	59.18	17.41	16.32	$C_{4.974}H_{10.41}NO_{7.84}$	Present study
Dunaliella sp.	NSCME	19.8	36.42	4.89	5.83	51.35	17.17	16.09	$C_{7.288}H_{11.66}NO_{7.72}$	Present study

HHV: High heating value; LHV: Low heating value; NSCME: Nutrient supplemented coal mine effluent; ND: Not detected.

However, a low lipid is observed in marine microalgae, *C. vulgaris* and *Dunaliella* sp. as 20.4% and 19.8%, respectively. The HHV of biomass ranged from 16.25–18.60 MJ Kg^{-1} and LHV of biomass ranged from 15.13–17.14 MJ Kg^{-1}, respectively (Table 3.4). Amongst fresh and marine microalgae, *C. pyrenoidosa* showed maximum HHV (18.60 MJ Kg^{-1}) and maximum LHV (17.14 MJ Kg^{-1}). In strong agreement with previously reported studies, microalgae accumulating high value metabolites like higher level lipids have high HHV (Pandey et al., 2019).

3.3.3.1 One-way ANOVA and Spearman's rank correlation for fuel characteristic variables

The proximate and ultimate fuel characteristic variables were statistically analyzed using one-way ANOVA and summarized in Table 3.5. The one-way ANOVA shows excluding mineral matter; all fuel characteristic variables are statistically significant with a p-value ≤ 0.001. The mineral matter is also statistically significant, with a p-value of 0.008. The F values of fuel ratio and HHV are estimated as 546.02 and 39.87, respectively, with a p-value < 0.001.

Table 3.5 One-way ANOVA for microalgae fuel characteristic variables.

Variables	Source of variation	SS	MS	*F*	*p*-value
Proximate analysis variables					
Moisture content	Between different microalgae groups	35.64	8.91	31.26	< 0.001
Volatile matter		97.68	24.42	139.87	< 0.001
Fixed carbon		119.61	29.90	1149.86	< 0.001
Ash		34.81	8.70	187.49	< 0.001
Mineral matter		45.49	11.37	6.28	0.008
Pyrite		100.87	25.21	30.18	< 0.001
Fuel ratio		0.13	0.03	546.02	< 0.001
HHV		11.66	2.92	39.87	< 0.001
Ultimate analysis variables					
C/H		18.68	4.67	11.08	0.001
O/C		3.81	0.95	74.43	< 0.001

All responses were observed at degree of freedom 4 and *F* critical 3.48; SS: sum of squares; MS: mean square.

Spearman's rank correlation is a linear correlation analysis based on the rank of two selected variables. The wide applicability of Spearman correlation statistics lies in the fact

of requiring fewer data conditions than the overall distribution pattern of the original variables (Meng et al., 2023). The correlation coefficient near 1 or –1 shows strong correlations between selected variables. Oppositely, a correlation coefficient close to 0 indicates a weaker correlation. In the present study, Spearman's rank correlation analysis was used to identify the greater influential factors among different proximate variables which impact fuel ratio and HHV significantly. Table 3.6 summarizes Spearman's rank correlation estimation for different microalgae fuel characteristics.

Table 3.6 Spearman's rank correlation estimation for different microalgae fuel characteristics.

	Fuel ratio			HHV		
Variables	r_s	***T* statistic**	***p*-value**	r_s	***T* statistic**	***p*-value**
CPY[c]						
Fixed carbon	0.72	2.89	0.01	0.63	2.42	0.03
Volatile matter	-0.16	0.45	0.03	-0.30	0.90	0.19
Ash	-0.49	1.63	0.05	-0.29	0.98	0.03
CM[d]						
Fixed carbon	0.64	2.38	0.02	0.48	1.61	0.05
Volatile matter	-0.96	9.76	< 0.001	-0.81	3.91	0.002
Ash	-0.48	1.0	0.05	-0.48	0.17	0.05
CPR[e]						
Fixed carbon	0.88	5.20	< 0.001	0.89	5.32	< 0.001
Volatile matter	-0.74	3.15	0.007	-0.33	1.05	0.17
Ash	-0.45	1.41	0.09	-0.49	0.62	0.50
CV[f]						
Fixed carbon	0.83	4.26	0.001	0.83	4.26	0.001
Volatile matter	-0.16	0.45	0.03	-0.04	0.35	0.48
Ash	-0.69	2.74	0.01	-0.22	0.63	0.27
DU[g]						
Fixed carbon	0.78	3.47	0.004	0.88	5.43	< 0.001
Volatile matter	-0.87	4.97	< 0.001	-0.021	0.36	0.36
Ash	-0.46	0.46	0.03	-0.26	0.76	0.23

HHV: High heating value; r_s: Spearman's rank correlation coefficient; CPY: *Chlorella pyrenoidosa*; CM: *Chlorella minutissima* ; CPR: *Chlorella protothecoides*; CV: *Chlorella vulgaris*; DU: *Dunaliella sp.*

Except for *C. minutissima*, all microalgae sp. showed a significant positive correlation between fixed carbon and fuel ratio with an absolute value of correlation coefficient of 0.7–0.88. However, the correlation coefficient is a positive moderate value (0.64) for *C. minutissima*. For both types of fresh and marine microalgae, the correlation between fixed carbon and fuel ratio is considered statistically significant based on $p \leq 0.05$.

For different microalgae sp., volatile matter and ash negatively correlate with fuel ratio. A statistically significant ($p \leq 0.05$) positive correlation between fixed carbon and HHV can be observed for all microalgae species. However, volatile matter or ash negatively correlates to HHV with $p \geq 0.05$. Based on Spearman's rank correlation coefficient and *p*-value, fixed carbon is identified as the most influential factor over volatile matter and ash content to impact fuel ratio and HHV, which is also reported in existing literature (Jankovic et al., 2020).

3.3.4 Fourier transform infrared spectroscopy analysis

The infrared spectra of five different microalgae sp. (fresh and marine sp.) showed little variation, as shown in Fig. 3.4. The identical peaks in FTIR spectra of microalgae sp. confirm similar functionality with minimal differences. The FTIR spectra peaks at 595 cm^{-1} and 665 cm^{-1} were assigned for deformation in the hydroxyl group (Peng et al., 2015).

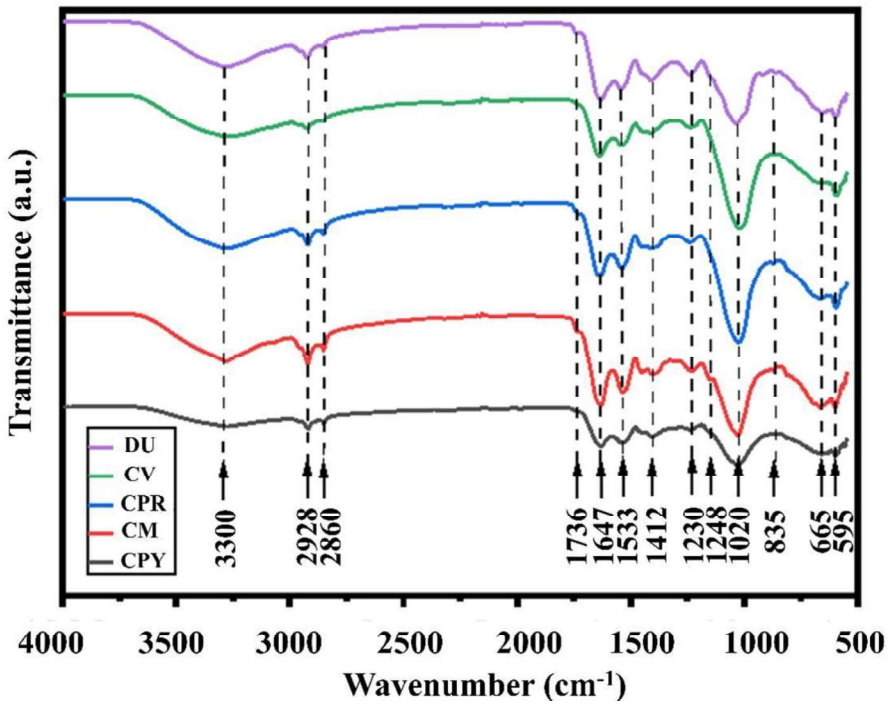

Fig. 3.4 FTIR spectrum of de-oiled microalgae. CPY: *Chlorella pyrenoidosa*; CM: *Chlorella minutissima*; CPR: *Chlorella protothecoides*; CV: *Chlorella vulgaris*; DU: *Dunaliella* sp.

In agreement with other studies, the prominent peak at 1647 cm^{-1} confirms carbonyl group C=O) stretching in amide-I bonds, while N-H bending and C-N stretching at 1533 cm^{-1} describe the amide- II bond (Gai et al., 2015). Similarly, the peak at 1736 cm^{-1} describes the symmetrical stretching of C=O of the ester functional group from lipids and fatty acids. Two subsequent peaks at 2860 cm^{-1} and 2928 cm^{-1} are assigned for symmetrical and asymmetrical stretching vibrations of CH_2 (Kocer and Ozcimen, 2022). Multiple small peaks at 3100–2800 cm^{-1} describe -CH_2 stretching in lipids. Additionally, frequent small peaks in the 1200–900 cm^{-1} region are assigned for stretching C-C, C-O-C, C-C, and C-O-P, confirming the presence of non-fibrous carbohydrates (Peng et al., 2015). The two medium bending peaks at 835 and 694 cm^{-1} are assigned for C=C alkene functional group (Ong et al., 2020).

3.3.5 Thermal decomposition behavior of microalgae

The TG-DTG curves for the thermal decomposition of different fresh and marine microalgae species (*C. pyrenoidosa*, *C. minutissima*, *C. protothecoides*, *C. vulgaris* and *Dunaliella sp.*) are presented at a heating rate of 10 ºC/min (Fig. 3.5).

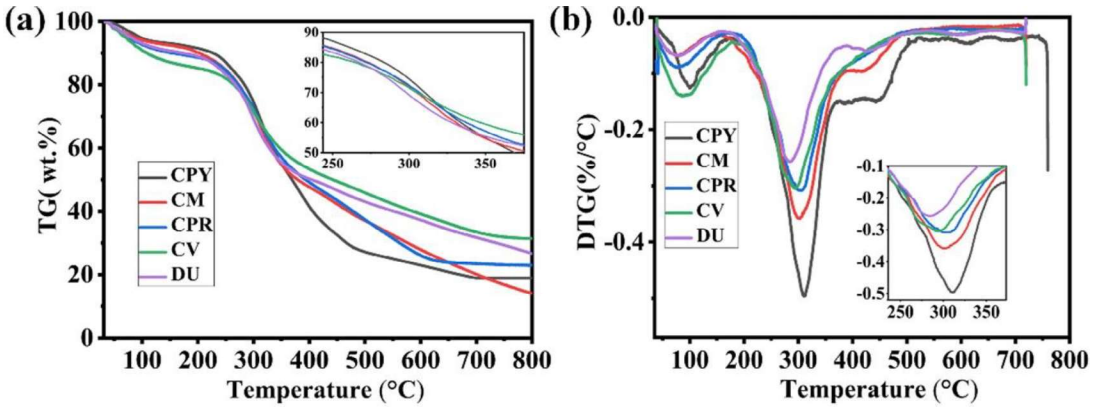

Fig. 3.5 Thermal analysis (a) TG curves (b) DTG curves of pyrolysis of de-oiled microalgae at the heating rate of 10 ºC/min. CPY: *Chlorella pyrenoidosa*; CM: *Chlorella minutissima*; CPR: *Chlorella protothecoides*; CV: *Chlorella vulgaris* and DU: *Dunaliella* sp.

Based on the defined trend of TG-DTG curves, the thermal decomposition during slow pyrolysis can be divided into three main temperature stages: ambient temperature to 200 ºC (first stage), 200–600 ºC (second stage) and 600–800 ºC (final stage) (Postawa et al., 2022). The first stage is responsible for evaporating unbound moisture from raw microalgae samples. The second stage defines the pyrolysis process, which is further divided into the first sub-stage (230–370 ºC), which corresponds to main pyrolysis and the second sub-stage (370–600 ºC) shows the passive pyrolysis. The greatest thermal decomposition of biomass compositions as cellulose and hemicellulose degradation is completed in the main pyrolysis stage, followed by the decomposition of carbonaceous materials as lignin in passive pyrolysis (Agbulut et al., 2023). The final third stage (600–800 ºC) corresponds to char production.

3.3.5.1 Effect of heating rate upon microalgae thermal decomposition

The TG and DTG experiments were conducted at three different heating rates of 10 –30 ºC/min to investigate the impact of heating rate upon microalgae thermal decomposition. The TG and DTG curves for the slow pyrolysis of selected microalgae are presented in Fig. 3.6 and Fig. 3.7, respectively. It can be observed that the complete mass loss during the pyrolysis was shifted to higher temperature zones with increasing heating rates. Increasing heating rate from 10–30 ºC/min positively increases ignition temperature (Ti) from 5–19 ºC for freshwater microalgae species and little variation of Ti (1–1.6 ºC) for marine microalgae species (Fig. 3.6). However, burnout temperature (Tb) is increased by 5–29 ºC for freshwater microalgae species and 18–19 ºC for marine microalgae species (Fig. 3.7). Similar to TG curves, in DTG, it is observed that peak temperature (Tp) is increased from 29–38 ºC for freshwater microalgae species and 27–36 ºC for marine microalgae (Fig. 3.7). The extension of Ti, Tp, and Tb may be understood by increased

thermal gradient throughout the cross-section of the sample which affects heat transfer between reactor and sample.

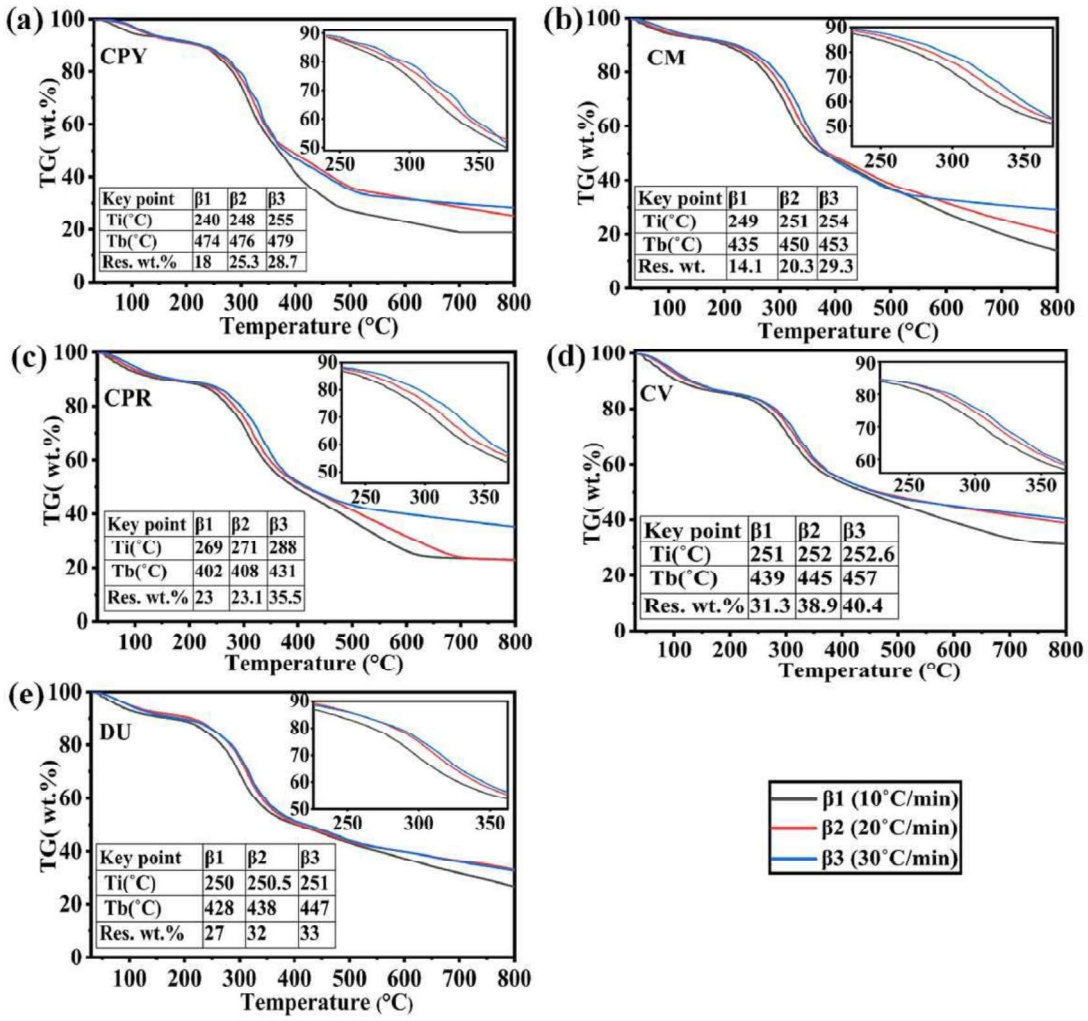

Fig. 3.6 TG curves for the pyrolysis of de-oiled microalgae at the heating rate of 10, 20 and 30 ºC/min (a) *Chlorella pyrenoidosa* (CPY) (b) *Chlorella minutissima* (CM) (c) *Chlorella protothecoides* (CPR) (d) *Chlorella vulgaris* (CV) (e) *Dunaliella sp.* (DU).

Further, increasing the heating rate results shorter residence time of biomass combustion within the reactor with an increased residual weight of nearly 10–15 % for freshwater microalgae species (*C. pyrenoidosa*, *C. minutissima* and *C. protothecoides*) and 6–9 % for marine microalgae species (*C. vulgaris*, *Dunaliella sp.*). The raw material composition of any microalgae species plays a major role in determining the extent of thermal decomposition. As per reported studies, carotenoids, lutein and β-carotene are

major compositions of marine microalgae such as *Dunaliella* sp.. However, freshwater microalgae mainly comprise proteins, lipids and non-fibrous carbohydrates (Ong et al., 2020). Further, it is observed that the maximum decomposition rate is increased in the range of 0.04–0.06 wt.%/ ºC for fresh microalgae species and 0.03 wt.%/ ºC for marine species at a heating rate increment from 10–30 ºC/min (Fig. 3.7). Similar level of heating rate effect is also observed in thermal decomposition of different microalgae biomass such as *C. vulgaris* (Chen et al., 2022), *N. occulta* (Kocer and Ozcimen, 2022) and *S. platensis* (Gai et al., 2015).

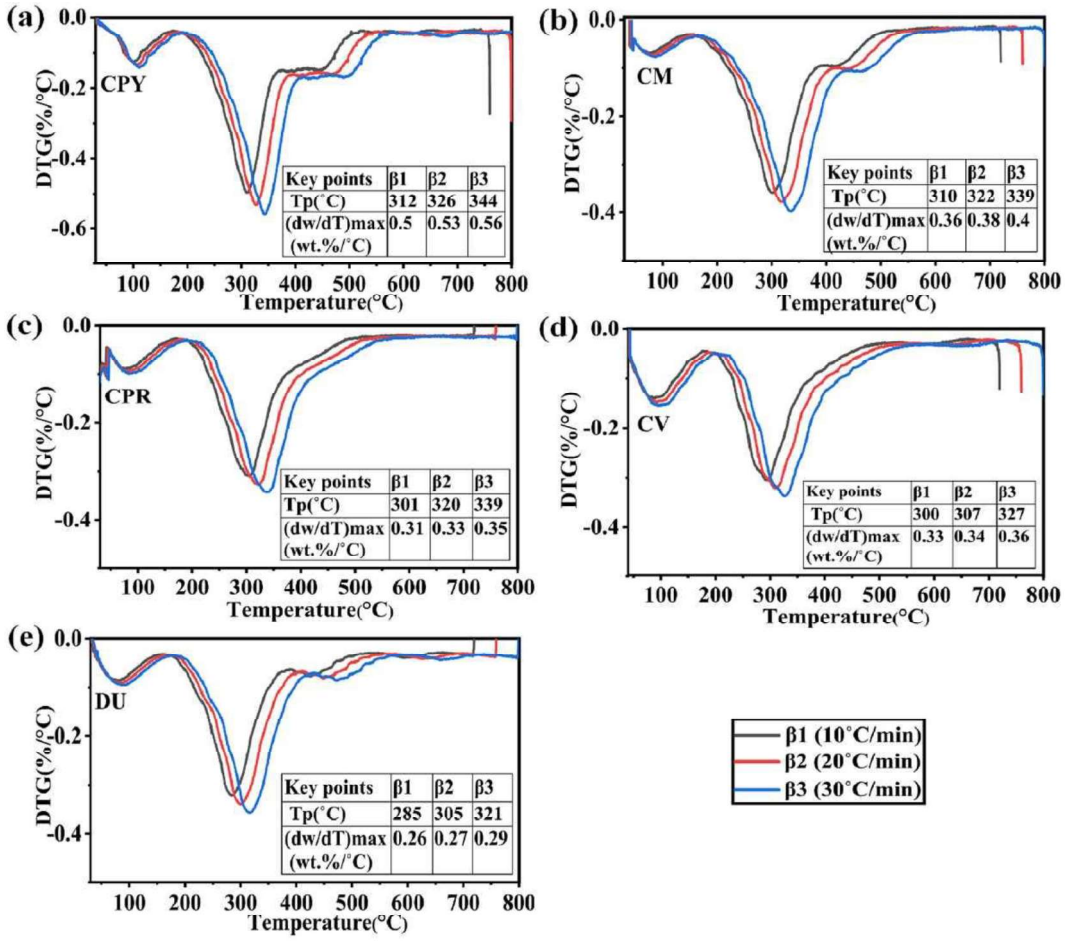

Fig. 3.7 DTG curves for the pyrolysis of de-oiled microalgae at the heating rate of 10, 20 and 30 ºC/min (a) *Chlorella pyrenoidosa* (CPY) (b) *Chlorella minutissima* (CM) (c) *Chlorella protothecoides* (CPR) (d) *Chlorella vulgaris* (CV) (e) *Dunaliella sp.* (DU).

The pyrolysis of *Dunaliella sp.* showed 0.26 %/ ºC minimum DTG max with a high residual mass of 27%. Similar to *Dunaliella sp.*, low DTG max (0.33%/ ºC) and high residual mass (31.3%) are also observed for *C. vulgaris*. A higher ash content of 21.63% and 20.57% is observed for marine microalgae species, *Dunaliella sp.* and *C. vulgaris,* respectively, compared to fresh microalgae species of *C. pyrenoidosa* (18% ash content). It is predicted that increasing the heating rate inside the reactor propagates higher heating flux across the biomass material, which leads to enhanced thermal decomposition (Shuping et al., 2010). Consequently, an increased heating rate may overcome intraparticle resistances by enhancing heat and mass transfer across the biomass particles within the reactor and lead to higher conversion levels (Shuping et al., 2010).

3.3.6 Kinetic analysis of freshwater and marine microalgae species

In the sequence of thermal behavior interpretation by TG-DTG trends, the pyrolysis characteristics were applied to calculate the thermal kinetics of both types of microalgae species by using the model-fitted CR approach and model-free DAEM method.

3.3.6.1 Coats Redfern method

Following model-fitted CR approach, eight models, three based on chemical reaction, three on diffusion and two on the Avraami Erofeev equation were examined (Table 3.1). As per earlier discussion, the thermal decomposition from 230–370 ºC is the main pyrolysis stage. The estimated values of E_a, A and R^2 corresponding to the main pyrolysis stage for the heating rate of 10 ºC/min are highlighted in Table 3.7. Experimental data fitting in CR Eq. (1) provides linear expression between $\ln(g(\alpha)/T^2)$ and 1/T with a value of slope as $– E_a/R$ and intercept as A.

The selection of CR model is decided in agreement with previous studies to systematize the data sets of selected models using the model selection approach (Postawa

et al., 2022). Firstly, all non-physical values as negative, zero, and near to zero would be rejected as essential selection standards. Secondly, R^2 should be near to one. Hence, all models with R^2 less than 0.98 would be rejected directly. The final selection decision would be based on validating model-fitted CR equation outcomes with model-free DAEM results. Thermal properties such as E_a and A are directly related to pyrolysis material and decomposition reactivity (Raza et al., 2022). Among different CR models, the N1 and N2 based on random nucleation and nuclei growth are rejected directly due to very poor accuracy with R^2 varied as 0.773–0.976 and E_a in the range of 1.91–10.74 kJ/mol, which is not consistent with the data outputs of other models. In chemical reaction models, varying nature of linearity with R^2 value 0.961–0.991 is observed for different O1, O2 and O3 models (Table 3.7). The first order reaction models (O1) showed comparatively less E_a for *C. vulgaris* (8.29 kJ/mol) and *C. pyrenoidosa* (9.61 kJ/mol) than other microalgae species *C. minutissima*, *C. protothecoides* and *Dunaliella sp.* (24.69–30.95 kJ/mol). Similar to other reported studies, increasing E_a is observed with increasing reaction order (for O2 and O3) (Postawa et al., 2022).

In the pyrolysis of *C. pyrenoidosa*, *C. minutissima*, *C. protothecoides*, *C. vulgaris* and *Dunaliella sp.*, the highest R^2 is observed for diffusion models (Fig. 3.8). Among different diffusion models, D3 showed the best linearity with R^2 of 0.99 for *C. pyrenoidosa*, *C. minutissima*, *C. vulgaris* and *Dunaliella sp.* (Fig. 3.8). However, for *C. protothecoides* diffusion model D2 is more acceptable than D3. Fig. 3.9 represents the visualization of different CR model acceptability orders. In agreement with other reported studies of biomass pyrolysis kinetics, higher E_a and correspondingly, higher A was observed for diffusion models than other mechanism models. The diffusion mechanism shows more dominant behavior than chemical reaction kinetics for a similar feedstock of other biomass, such as date palm fibers (Raza et al., 2022) and agriculture waste (Naqvi et al., 2019). The

reliability and consistency of the diffusion mechanism are based on biomass decomposition within the pyrolysis reactor through molecular diffusion rather than a typical reaction. Among selected microalgae species, the best-fitted CR models show E_a of *C. protothecoides* as a minimum with a value of 49.9 kJ/mol, followed by *C. pyrenoidosa*, *C. vulgaris*, *C. minutissima* and *Dunaliella sp.* with E_a of 53.87, 54.04, 57.13 and 65.82 kJ/mol respectively. Despite of R^2 value of 0.99, in the case of *C. protothecoides*, D2 over O3, and in *Dunaliella sp.*, D3 over O2 is considered more suitable after DAEM validation (Fig. 3.9).

Table 3.7 Kinetic parameter calculation of microalgae at main pyrolysis stage (230 – 370 ºC) using different reaction models of Coats Redfern method.

Samples	Model name	Regression coefficient (R^2)	Activation energy (E_a– kJ/mol)	Frequency factor (A – s^{-1})
CPY	O1	0.961	9.61	6.77×10^{2}
	O2	0.984	37.16	1.29×10^{4}
	O3	0.983	46.75	3.62×10^{4}
	D1	0.976	43.73	2.38×10^{4}
	D2	0.980	48.55	4.97×10^{4}
	D3	0.991	53.87	5.57×10^{4}
	N1	0.947	7.89	5.57
	N2	0.773	2.11	0.55
CM	O1	0.987	26.19	5.86×10^{2}
	O2	0.986	33.94	5.74×10^{3}
	O3	0.981	42.79	4.42×10^{4}
	D1	0.989	48.52	4.85×10^{4}
	D2	0.990	52.59	5.03×10^{4}
	D3	0.991	57.13	5.85×10^{4}
	N1	0.971	8.36	5.29
	N2	0.865	2.43	0.54
CPR	O1	0.990	24.69	0.4×10^{3}
	O2	0.993	36.47	4.64×10^{3}
	O3	0.996	40.32	2.69×10^{4}
	D1	0.983	22.49	1.82×10^{4}
	D2	0.992	49.88	3.11×10^{4}
	D3	0.981	54.04	7.02×10^{4}
	N1	0.973	7.56	4.058
	N2	0.852	1.91	0.39
CV	O1	0.978	8.29	1.30×10^{2}
	O2	0.981	23.09	1.78×10^{3}
	O3	0.971	37.68	2.98×10^{3}
	D1	0.984	33.75	2.14×10^{3}
	D2	0.985	38.24	3.0×10^{3}
	D3	0.991	54.04	3.44×10^{3}
	N1	0.926	4.60	3.71×10^{-7}
	N2	0.857	2.31	1.54×10^{-7}

Samples	Model name	Regression coefficient (R^2)	Activation energy (E_a– kJ/mol)	Frequency factor (A – s^{-1})
DU	O1	0.990	30.95	10.32
	O2	0.993	40.19	2.27×10^4
	O3	0.990	50.85	2.76×10^5
	D1	0.983	55.70	3.20×10^5
	D2	0.988	60.44	3.92×10^5
	D3	0.993	65.82	4.44×10^5
	N1	0.976	10.74	10.97
	N2	0.854	4.01	1.14

CPY: *Chlorella pyrenoidosa*; CM: *Chlorella minutissima*; CPR: *Chlorella protothecoides*; CV: *Chlorella vulgaris* and DU: *Dunaliella* sp.

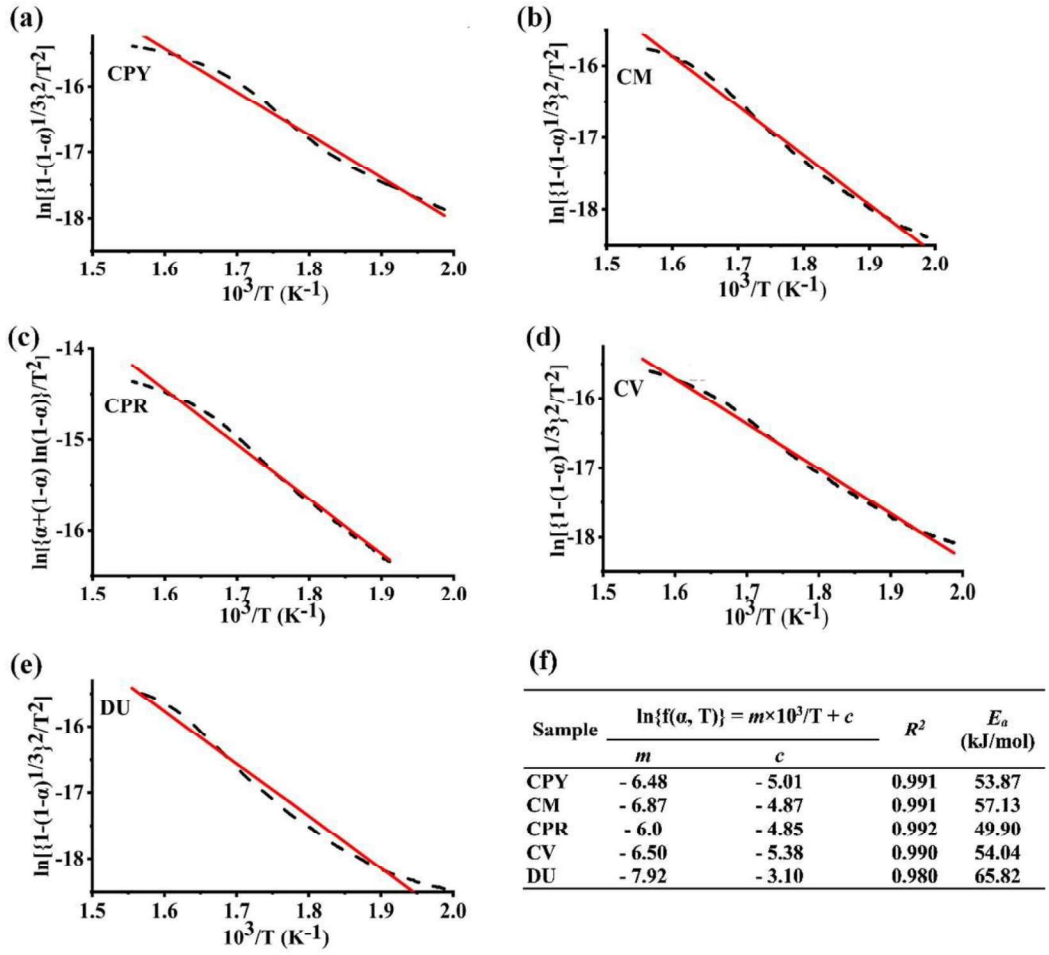

(f)

Sample	$\ln\{f(\alpha, T)\} = m\times10^3/T + c$		R^2	E_a (kJ/mol)
	m	*c*		
CPY	- 6.48	- 5.01	0.991	53.87
CM	- 6.87	- 4.87	0.991	57.13
CPR	- 6.0	- 4.85	0.992	49.90
CV	- 6.50	- 5.38	0.990	54.04
DU	- 7.92	- 3.10	0.980	65.82

Fig. 3.8 Best fitted Coats Redfern kinetic models based on solid state diffusion for main pyrolysis stage (230–370 ºC) of de-oiled microalgae. (a) *Chlorella pyrenoidosa* (CPY), (b) *Chlorella minutissima* (CM), (c) *Chlorella protothecoides* (CPR), (d) *Chlorella vulgaris* (CV), (e) *Dunaliella sp.* (DU) (f) Regression coefficient (R^2) and activation energy (E_a) estimation.

3.3.6.2 Distributed activation energy model approach

The present study applied a model-free DAEM approach to estimate the E_a of fresh and saline microalgae species. The DAEM model validates the output data sets of different CR models for comparative kinetic analysis.

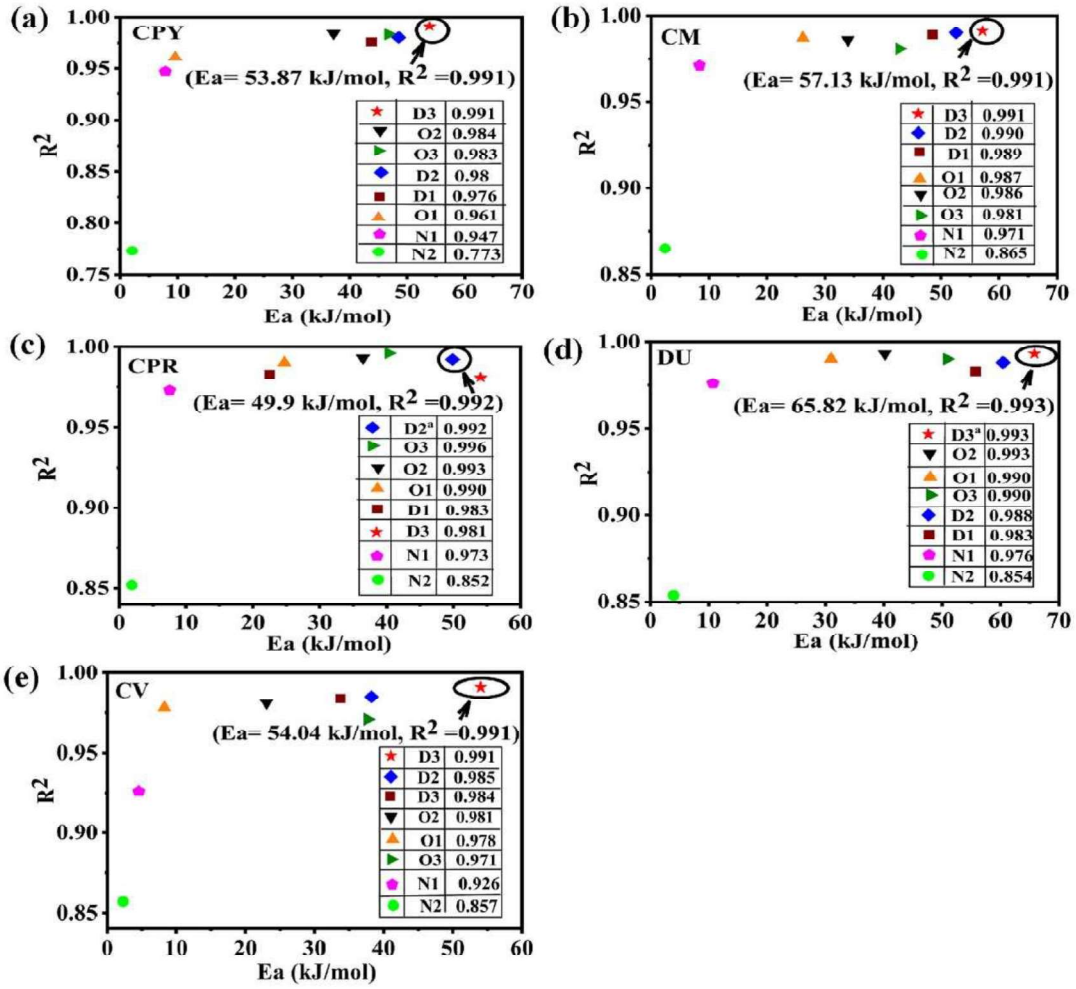

Fig. 3.9 Acceptability order of Coats Redfern kinetic models based on coefficient of determination (R^2) for different de-oiled microalgae species (a) *Chlorella pyrenoidosa* (CPY) (b) *Chlorella minutissima* (CM) (c) *Chlorella protothecoides* (CPR) (d) *Chlorella vulgaris* (CV) (e) *Dunaliella sp.* (DU). ([a]Validated with DAEM models).

Three TGA data set at 10–30 ºC/min heating rates were utilized for the pyrolysis kinetics study. The mass conversion ratio of 0.1 and 0.9 with a unit step increment of 0.1 was applied for the total mass loss of biomass during pyrolysis. The independent linearly fitted parallel lines follow first-order reactions with altered E_a at different conversion states.

As the most successful approach to studying complex biomass pyrolysis, kinetic parameter calculation of model-free DAEM method is presented for different microalgae species. The R^2 was observed to be higher than 0.95 for all microalgae samples. In the DAEM approach, E_a distribution over a range of mass conversion ratio (α) was represented by Fig. 3.10. The E_a value of de-oiled microalgae samples varies greatly with an increment of conversion fractions (α = 0.1–0.9). In agreement with other reported DAEM studies of biomass thermal kinetics, E_a initially increased significantly with a conversion ratio of 0.1 to 0.4. Afterward, E_a changes gradually near to 0.7 mass conversion ratio. Then sharp uptrend can be visualized with maximum E_a at a conversion ratio of 0.9 for all studied microalgae species, as shown in Fig. 3.11a.

The different E_a at different conversion ratios indicates the bond strength variation of a biomolecule at different stages of the pyrolysis process (Shuping et al., 2010). The apparent E_a corresponding to complete biomass pyrolysis was observed as 55.87±11.16, 56.09±6.32, 46.58±5.55, 55.26±13.14 and 68.09±10.62 kJ/mol for *C. pyrenoidosa*, *C. minutissima*, *C. protothecoides*, *C. vulgaris* and *Dunaliella sp.*, respectively. The E_a calculated by the present study is compared with other reported studies in the literature, as shown in Table 3.8.

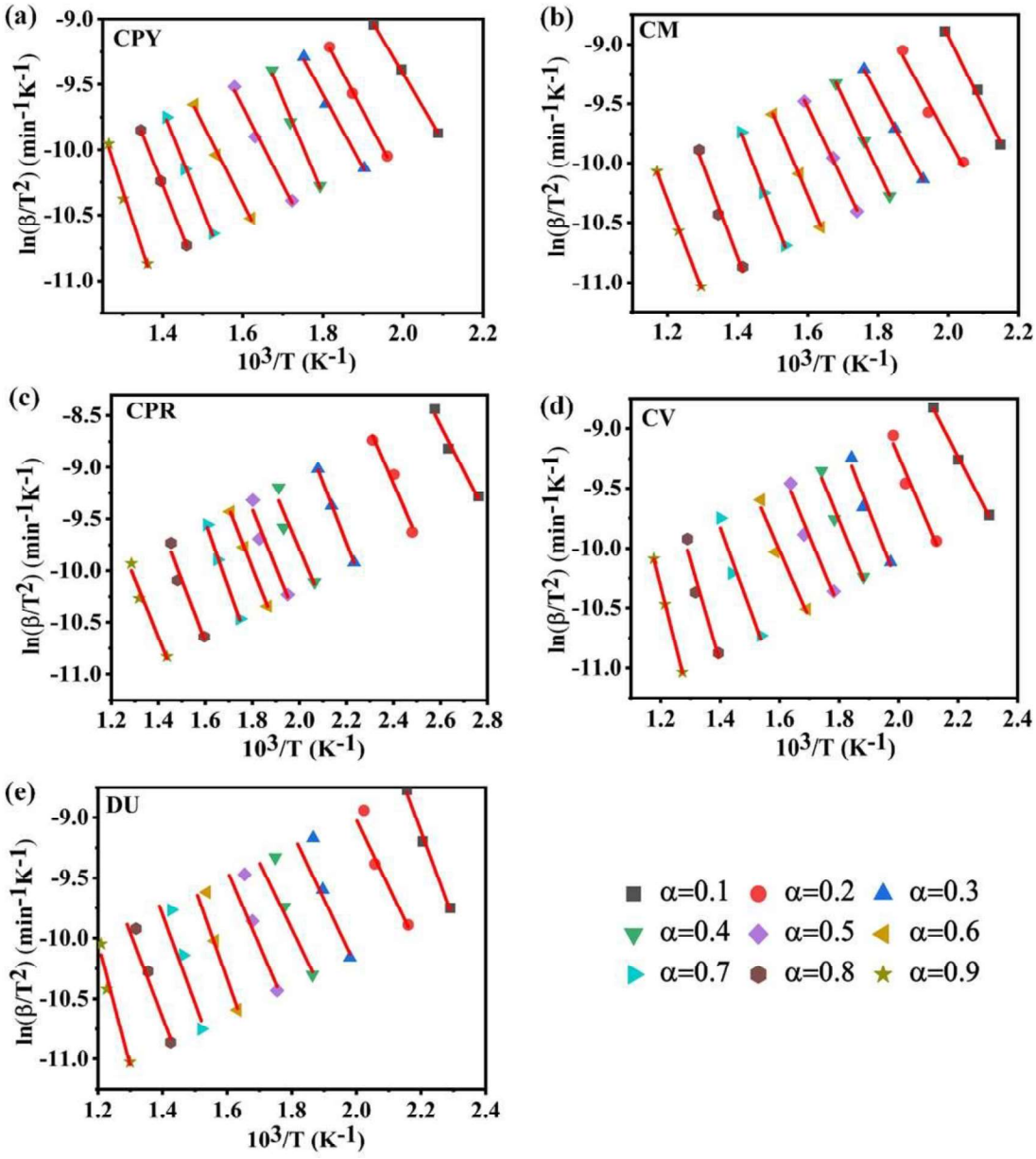

Fig. 3.10 Distributed activation energy model (DAEM) of (a) *Chlorella pyrenoidosa* (CPY) (b) *Chlorella minutissima* (CM) (c) *Chlorella protothecoides* (CPR) (d) *Chlorella vulgaris* (CV) (e) *Dunaliella sp.* (DU) at a heating rate of 10, 20 and 30˚C/min for mass conversion ratio (α = 0.1– 0.9).

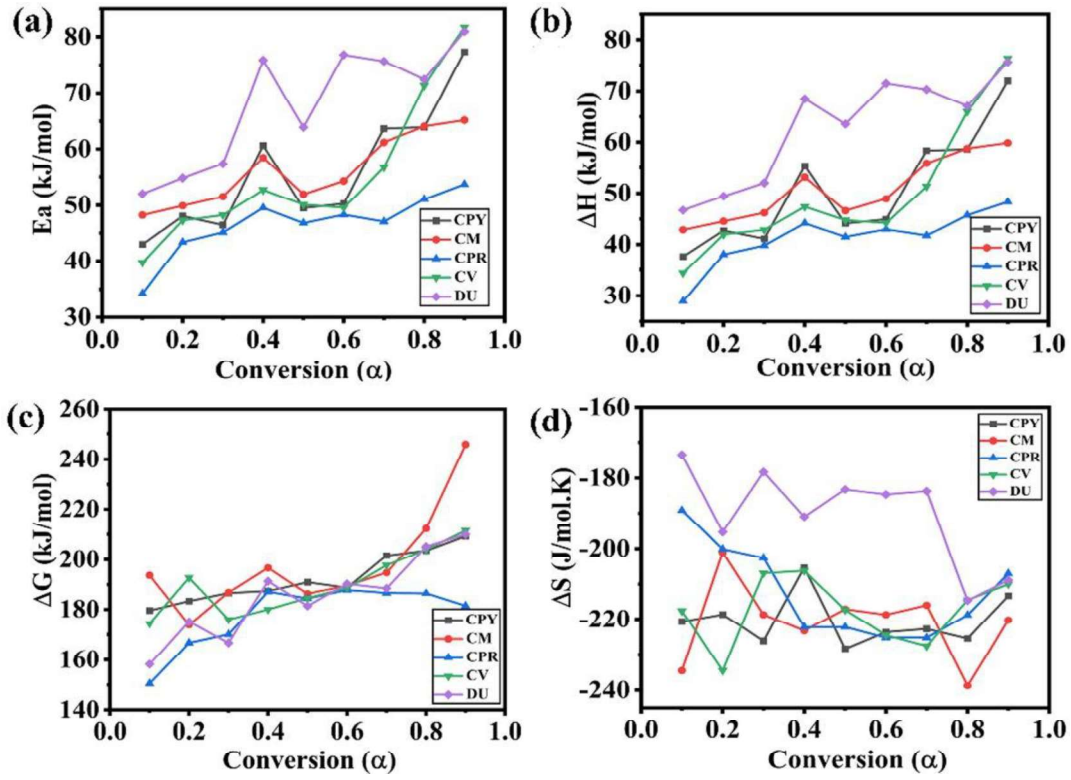

Fig. 3.11 Thermodynamic properties estimation of de-oiled microalgae (a) Activation energy (E_a) (b) Enthalpy change (ΔH) (c) Gibbs free energy change (ΔG) (d) Entropy change (ΔS) for mass conversion ratio (α=0.1–0.9). CPY: *Chlorella pyrenoidosa*; CM: *Chlorella minutissima*; CPR: *Chlorella protothecoides*; CV: *Chlorella vulgaris* and DU: *Dunaliella* sp.

Table 3.8 Comparison of activation energy calculated by present study with reported in the literature.

Study	Type of biomass	Applied method	E_a (kJ/mol)	References
Kinetics of waste plant biomass pyrolysis	Stalks, leaves and whole plant of Maize	Coats Redfern method	28.4, 30.6 and 33.0	(Postawa et al., 2022)
Thermo-kinetics and thermodynamic analysis of date palm surface fibers	Date palm surface fibers	Coats Redfern method	96 – 98	(Raza et al., 2022)
Combustion and pyrolysis of *C. vulgaris* using TGA analysis	*C. vulgaris*	KAS and FWO method	45 – 51	(Agrawal and Chakraborty, 2013)

Study	Type of biomass	Applied method	E_a (kJ/mol)	References
Combustion characteristics of low lipid microalgae	*Spirulina platensis*	Starink method	84.29	(Gai et al., 2015)
Pyrolytic characteristics of microalgae	*C. protothecoides and Spirulina platensis*	Freeman – Carroll method	42.2–52.5 and 76.2–97.0	(Peng et al., 2015)
Pyrolysis of residual microalgae cultivated in wastewater	Mixed cultivation of *Chlorella* sp. and *Bracteacoccus* sp.	Starink, KAS and FWO method	182–256	(Shahid et al., 2019)
Microwave-assisted pyrolysis characteristics of *Dunaliella salina*	*Dunaliella salina*	Coats Redfern method	66.84	(Chen et al., 2020)
Kinetic and thermodynamic properties of fresh and marine microalgae sp.	*C. pyrenoidosa*, *C. minutissima*, *C. protothecoides*, *C. vulgaris*, *Dunaliella sp.*	Coats Redfern and DAEM method	55.87±11.16 56.09±6.32 46.58±5.55 55.26±13.14 68.09±10.62	Present study

KAS: Kissinger- Akahira-Sunose; FWO: Flynn–Wall–Ozawa; DAEM: Distributed activation energy model.

3.3.6.3 Thermodynamic properties analysis

The thermodynamic properties such as ΔH, ΔG and ΔS for pyrolysis of different microalgae species were estimated by using both model-fitted (CR method) and model-free (DAEM) approaches (Table 3.9).

Table 3.9 Thermodynamic properties of different microalgae sp. at main pyrolysis stage (230–370 ºC) by applying Coats Redfern and DAEM method.

Sample	Calculation by Coats Redfern			Calculation by DAEM		
	ΔH (kJ/mol)	ΔG (kJ/mol)	ΔS (J/mol• K)	ΔH (kJ/mol)	ΔG (kJ/mol)	ΔS (J/mol•K)
CPY	50.52	190.09	– 0.22	50.52±11.16	192.29±10.08	– 0.22±0.006
CM	50.74	189.10	– 0.21	50.74±5.96	197.73±19.54	– 0.22±0.023
CPR	41.23	171.85	– 0.20	41.23±5.23	177.87±12.83	– 0.21±0.012
CV	49.91	187.34	– 0.21	49.91±13.13	189.90±11.99	– 0.21±0.009
DU	62.74	180.84	– 0.18	62.74±10.01	185.15±15.89	– 0.19±0.013

ΔH: Enthalpy change; ΔG: Gibbs free energy change; ΔS: Entropy change; CPY: *Chlorella pyrenoidosa*; CM: *Chlorella minutissima*; CPR: *Chlorella protothecoides*; CV: *Chlorella vulgaris*; DU: *Dunaliella sp.*

The thermodynamic properties of different biomass materials are summarized in Table 3.10. The variation of ΔH, ΔG and ΔS with mass conversion ratio (α=0.1 to 0.9) are shown in Fig. 3.11b–d.

Table 3.10 Summary of thermodynamic properties of different biomass materials.

Biomass material	ΔH(kJ/mol)	ΔG(kJ/mol)	ΔS (J/mol•K)	References
Microalgae (*Chlorella minutissima*)	37.15	161.22	– 0.23	(Kocer and Ozcimen, 2022)
Microalgae (*Botryococcus braunii*)	29.08	153.88	– 0.22	(Kocer and Ozcimen, 2022)
Microalgae (*Nannochloropsis oculata*)	16.27	160.06	– 0.27	(Kocer and Ozcimen, 2022)
Microalgae (*Tetraselmis suecica*)	23.65	151.47	– 0.23	(Kocer and Ozcimen, 2022)
Date palm surface fibers	93	205	– 0.30	(Raza et al., 2022)
Dry oil sludge	50	70	– 0.037	(Naqvi et al., 2019)
Bagasse	80.37	173.43	-0.15	(Naqvi et al., 2019)
Wheat straw	77.47	174.39	-0.16	(Naqvi et al., 2019)
Wood chip	85.17	175.43	-0.15	(Naqvi et al., 2019)
Microalgae (*Chlorella pyrenoidosa*)	50.52±11.16	192.29±10.08	-0.22±0.006	Present study

ΔH: Enthalpy change; ΔG: Gibbs free energy change; ΔS: Entropy change.

The ΔH values (heat absorbed or released by the system at fixed pressure) were positive with varying ranges between 41.23–62.74 (kJ/mol), considering both CR and DAEM approaches. At the initial conversion stages of pyrolysis, less ΔH was observed due to the comparatively easy decomposition of cellulose and hemicellulose; however, in later stages, ΔH value increased as more energy is required for lignin decomposition. In the previous study, higher ΔH is reported for pyrolysis of agriculture residues: bagasse (80.37 kJ/mol), wheat straw (77.47 kJ/mol), and wood chip (85.17 kJ/mol) (Naqvi et al., 2019). The ΔG is an effective tool to determine reaction energetics and spontaneity.

Similar to ΔH, the estimated ΔG for mass loss regions were positive in the 177.87–197.73kJ/mol range, which showed the endergonic or nonspontaneous nature of thermal pyrolysis. Compared to microalgal biomass, ΔG for slow pyrolysis of wood chips is reported as 175.43 kJ/mol (Naqvi et al., 2019). In addition to that, negative ΔS of 0.19–0.22 J/mol•K was observed during pyrolysis of different microalgae, which predicted better stability of thermally decomposed products rather than the initial reactant. A similar trend of ΔS was observed in thermal pyrolysis of other microalgae as *Tetraselmis suecica* (–0.23 J/mol• K) and *Nannochloropsis oculate* (–0.27 J/mol•K) (Kocer and Ozcimen, 2022). Oppositely, very low ΔS (– 0.037 J/mol•K) was reported for dry oil sludge pyrolysis (Ali et al., 2021). Dual validation of thermodynamic parameters by a model-fitted and model-free approach provided consistent data with high accuracy.

3.3.7 Thermal behavior prediction by Deep neural network (DNN) simulation

3.3.7.1 Optimization of the Conv 1D-LSTM model

Targeting the data discrepancy issue during frequent TGA investigations and to provide consistent TGA data for microalgae pyrolysis study, the Conv1D-LSTM model was developed. For model development, the TGA data set of pyrolysis temperature and heating rate was used as input parameters and residual mass % as an output parameter (Fig. 3.12). In previous studies, Sigmoid, Tansig, Relu and Tanh were applied as activation functions for ANN modeling (Tian et al., 2022). Activation functions help neural networks to learn complex patterns from the experimental data. PrelU was used as an activation function and Adam as an optimizer algorithm. Adam performs more efficiently with little memory requirement and can handle noisy and scattered gradients.

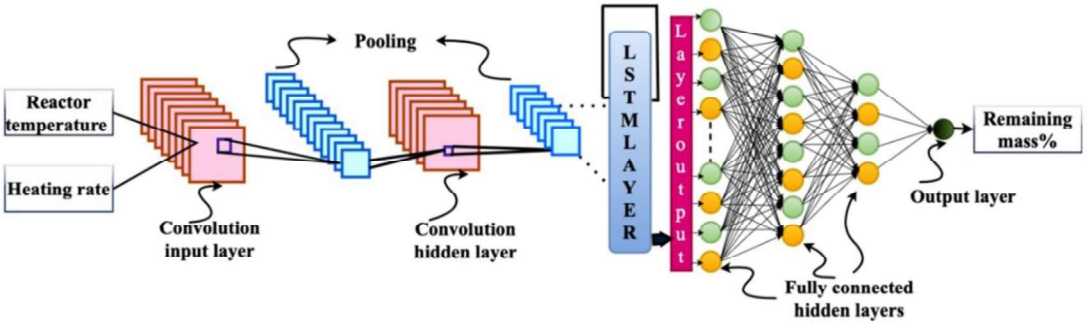

Fig. 3.12 Deep neural network architecture to predict thermal behavior of de-oiled microalgae *Chlorella pyrenoidosa*.

In this study of microalgae pyrolysis, total 7 DNN models were designed and the best predicted model was analysed by comparing different performance determining coefficients such as MSE, RMSE, R^2 and MAE (Eq. 3.16–3.19). Based on these coefficients, the best performing model was selected as DNN 6, which had 105 neurons in the form of 32-24-32*12*4*1 consisting of 6 layers. DNN 6 showed minimum MSE for all three heating rates as 3.91×10^{-6}, 2.00×10^{-6}, and 0.67×10^{-6} at 10, 20 and 30 ºC/min, respectively. In sequence, the best R^2 for the selected model is reported as 0.99779, 0.99826 and 0.99939 at heating rates of 10, 20 and 30 ºC/min, respectively (Table 3.11).

In the case of closely similar R^2, the real performance of models must be assessed by using error metrics than merely R^2 (Teng et al., 2019). Therefore, MSE, RMSE, and MAE must be considered along with R^2. The best suitable DNN6 model showed a minimum RMSE of 0.00198 and MAE of 0.00164 at a 10 ºC/min pyrolysis heating rate of *C. pyrenoidosa* (Table 3.11). In the previously reported ANN model of peanut shell and sewage sludge co-pyrolysis, 21 topologies were compared with a minimum RMSE of 0.35614 and a maximum R^2 of 0.99992 (Bi et al., 2021).

Table 3.11 The performance comparison of different deep neural network structure.

Model	Input parameter	Network topology[a]	Heating rate (ºC/min)	R^2	MSE (10^{-6})	RMSE	MAE
DNN1	Temperature and Heating rate	16-8-16*8*4*1	10	0.99547	7.20	0.00268	0.00225
			20	0.99870	1.33	0.00115	0.00082
			30	0.99876	1.53	0.00123	0.00092
DNN2		16-12-16*8*4*1	10	0.99688	6.34	0.00252	0.00201
			20	0.99828	2.16	0.00147	0.00108
			30	0.99610	4.57	0.00214	0.00164
DNN3		32-8-32*16*8*1	10	0.99526	8.09	0.00285	0.00217
			20	0.99852	1.67	0.00129	0.00103
			30	0.99808	1.68	0.00128	0.00107
DNN4		32-12-16*8*4*1	10	0.99354	10.48	0.00323	0.00224
			20	0.99550	6.13	0.00248	0.00177
			30	0.99408	6.55	0.00255	0.00233
DNN5		32-16-32*12*4*1	10	0.99577	6.86	0.00262	0.00179
			20	0.99832	1.75	0.00132	0.00109
			30	0.99788	2.97	0.00172	0.00129
DNN6		32-24-32*12*4*1	10	0.99779	3.91	0.00198	0.00164
			20	0.99826	2.00	0.00142	0.00128
			30	0.99939	0.67	0.00082	0.00069
DNN7		32-24-32*16*8*1	10	0.99578	6.62	0.00257	0.00217
			20	0.99602	4.77	0.00218	0.00171
			30	0.99819	2.18	0.00147	0.00123

DNN: Deep neural network; MSE: Mean square error; RMSE: Root mean square error; MAE: Mean absolute error; [a] represents convolution layer; *represents to fully connected hidden layer.

TG-FTIR investigation of municipal solid waste combustion by the DNN model showed R^2 as 0.9441 with a minimum MSE of 0.0265 for training loss and 0.0055 for validity loss at epoch 200 (Tian et al., 2022). The co-pyrolysis of coal slime with cattle manure showed R^2, MAE, and RMSE as 0.99998, 0.0983 and 0.1451, respectively (Jiang et al., 2022). In the thermal decomposition of *C. vulgaris*, the R^2 was found above 0.9950 using ANN modeling (Agrawal and Chakraborty, 2013). Co-pyrolysis of hazelnut husks with lignite coal shows 0.9994 R^2, 0.6240 RMSE and 0.4840 MAE (Yildiz et al., 2016). The present study confirms a very high level of accuracy with minimum MSE (in order of 10^{-6}) by using Conv1D-LSTM layers to simulate microalgae pyrolysis TG data, as shown in Fig. 3.13. The overlapping of experimental and predicted data in TG curves for all three heating rates (10–30 ºC/min) and exactness of training and validation loss from model loss

curves confirms the feasibility of Conv1D-LSTM model to simulate microalgae pyrolysis (Fig. 3.13).

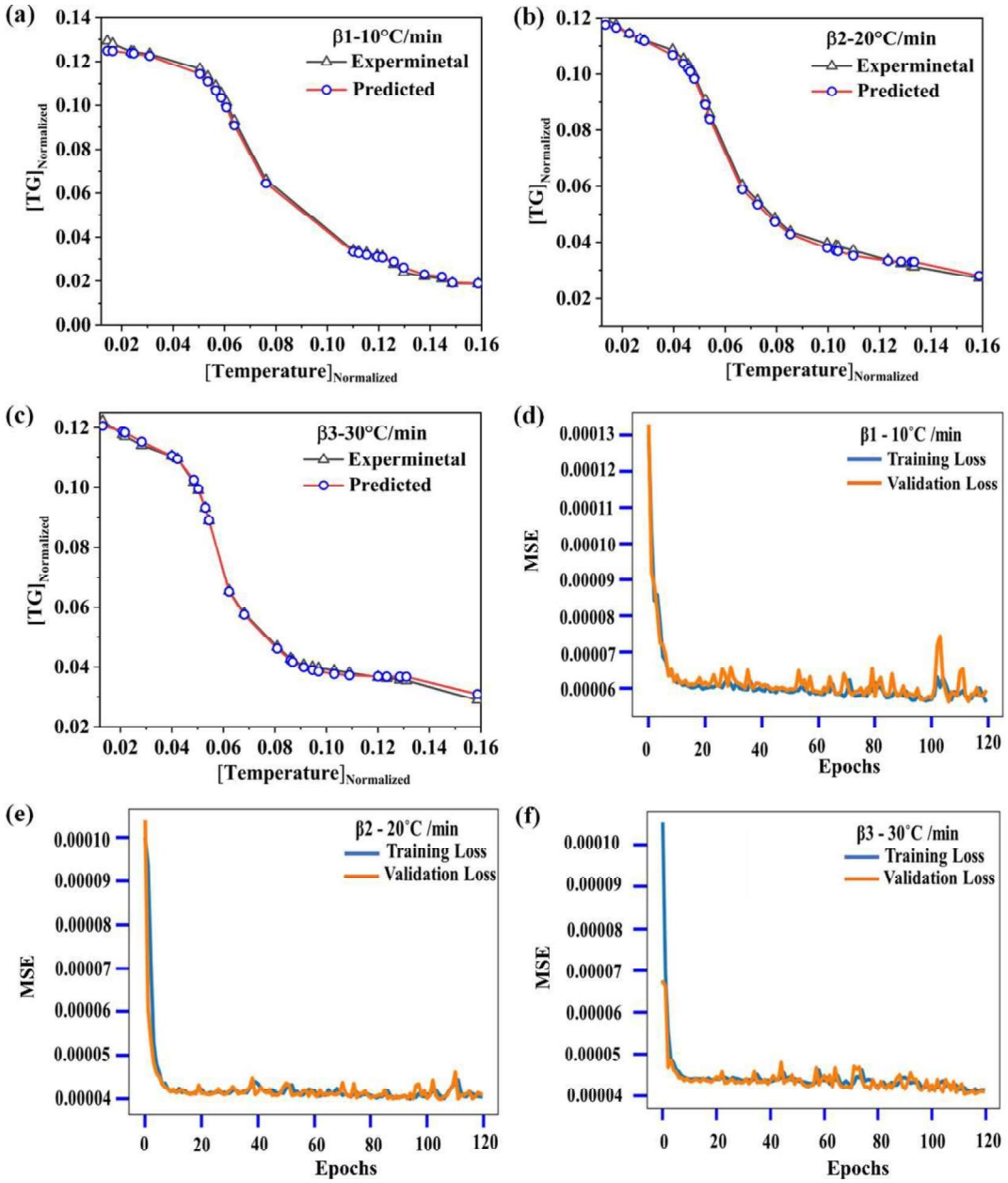

Fig. 3.13 Comparative assessment of experimental and predicted pyrolysis of de-oiled microalgae *Chlorella pyrenoidosa* at a heating rate (ºC/min) of (a) 10 (b) 20 (c) 30. Variation of training and validation loss with number of epochs at a heating rate (ºC/min) of (d) 10 (e) 20 (f) 30.

3.4. Conclusion

The present chapter outcomes indicate *C. pyrenoidosa* (NCIM 2738) can be considered as a candidate microalgae to treat and desalinate NSCME and considered as potential alternative biofuel feedstock for sustainable biofuel production. During 12 days batch cultivation in NSCME, *C. pyrenoidosa* showed maximum growth potential amongst all five, fresh and marine microalgae strains with μ_{net} of 0.33 d^{-1}. The microalgae *C. pyrenoidosa* performed excellent in NSCME with lipid content of 31.5 % (very close to maximum 32.6 % shown by *C. minutissima*) and associated with maximum nutrient removal efficiency in terms of EC (86.9 %) and COD (89.8 %).

Fuel characteristic analysis of fresh and marine microalgal biomass also conclude de-oiled *C. pyrenoidosa* as an appropriate pyrolysis feedstock with maximum HHV and LHV of 18.60 MJ Kg^{-1} and 17.14 MJ Kg^{-1} respectively. Further, model-fitted CR and model-free DAEM showed apparent E_a of *C. pyrenoidosa, C. minutissima, C. protothecoides, C. vulgaris and Dunaliella sp.* is 55.87±11.16, 56.09±6.32, 46.58±5.55, 55.26±13.14 and 68.09±10.62 kJ/mol respectively.

The thermodynamic parameters such as ΔH, ΔG and ΔS of studied microalgae are estimated in the range of 41.23–62.74 kJ/mol, 177.87–197.73 kJ/mol and 0.19–0.22 J/mol•K, respectively. At last, Conv1D-LSTM model is developed and used to predict microalgal thermal decomposition data. The best deep neural network model (DNN6) showed minimum MSE (10^{-6}) and high $R^2 > 0.997$ for 10, 20 and 30 ºC/min heating rates. Hence, systematic screening of microalgae encourages an integrated strategy to treat CME with bioenergy production using artificial intelligence application.